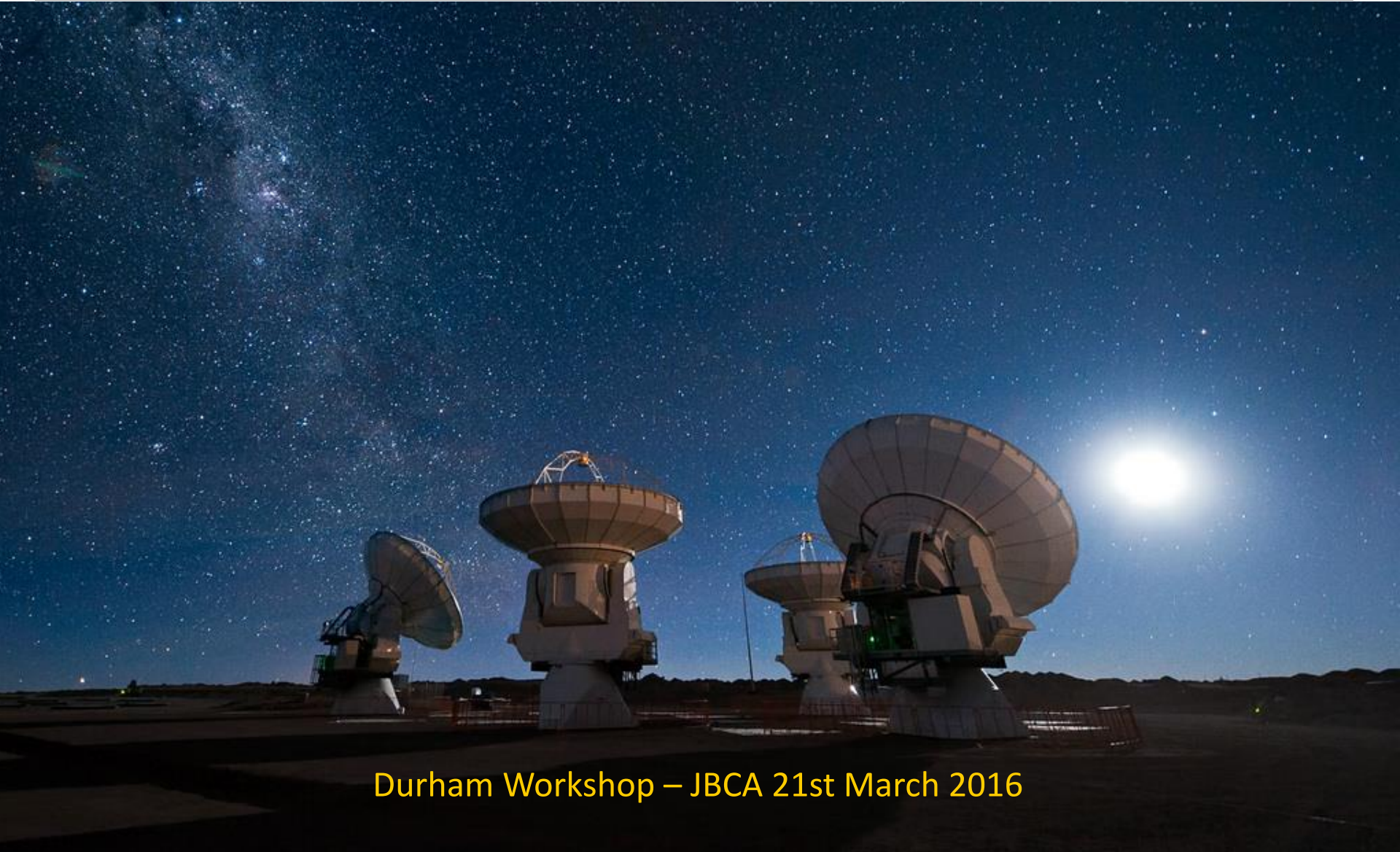


An Introduction To Interferometers

Tom Muxlow, JBCA



Durham Workshop – JBCA 21st March 2016

Outline

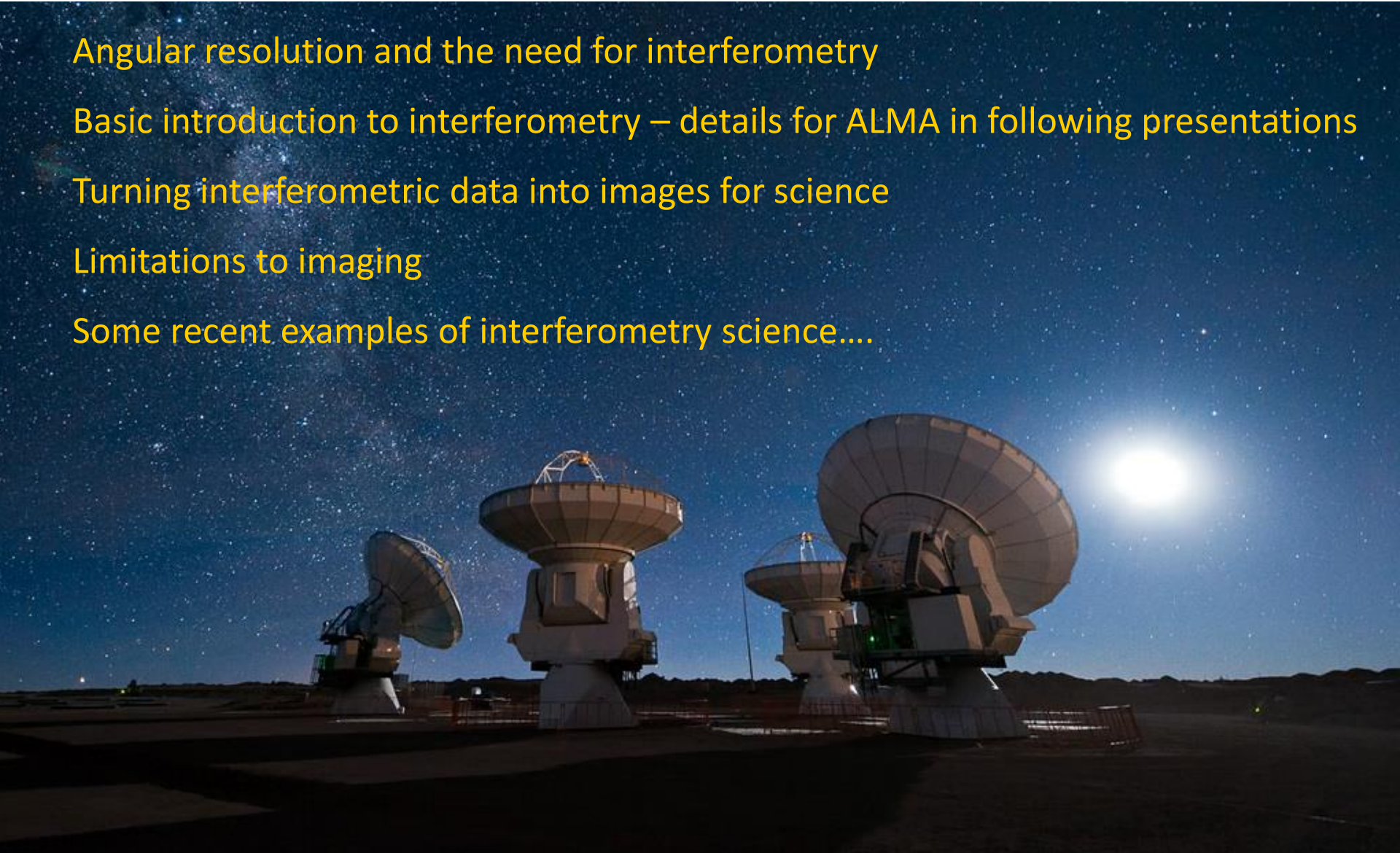
Angular resolution and the need for interferometry

Basic introduction to interferometry – details for ALMA in following presentations

Turning interferometric data into images for science

Limitations to imaging

Some recent examples of interferometry science....



Apertures – Angular resolution & psf

A fully filled aperture (diffraction-limited refracting telescope)

Samples image spatial frequencies out to a cut-off set by objective diameter



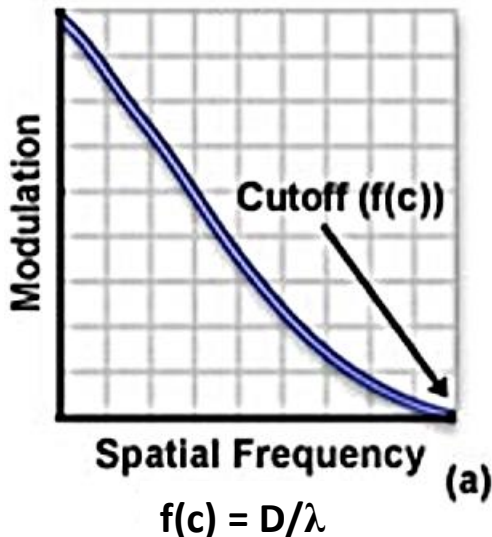
Image contrast (modulation) is highest at low spatial frequencies, decreasing to a value of zero as the spatial frequency increases $\rightarrow f(c)=D/\lambda$.

Resolution set by PSF 1st minimum $\rightarrow \theta=1.22\lambda/D$

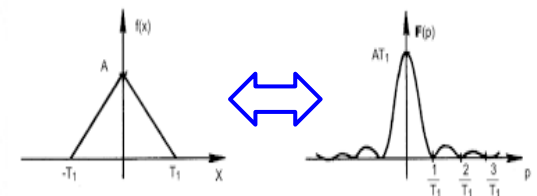
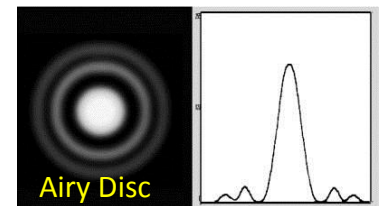
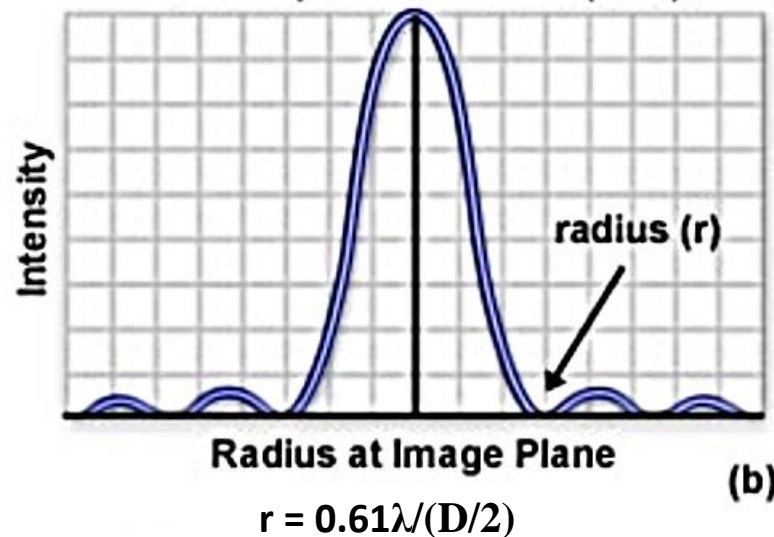
Fourier Relationship between MTF and PSF

MTF=Modulation Transfer Function

MTF



Point Spread Function (PSF)



PSF = FT of sampled spatial frequencies in the telescope aperture

Apertures – Angular resolution & psf

A fully filled aperture (diffraction-limited refracting telescope)

Samples image spatial frequencies out to a cut-off set by objective diameter

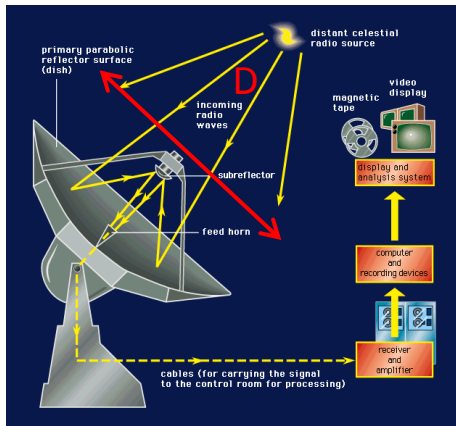
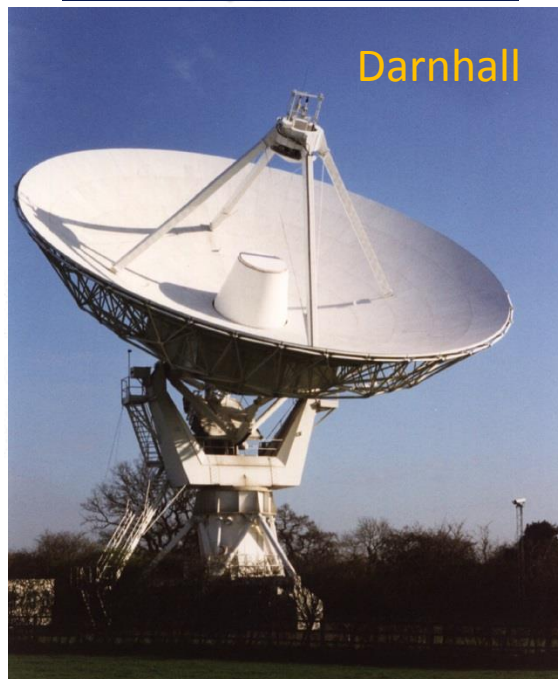
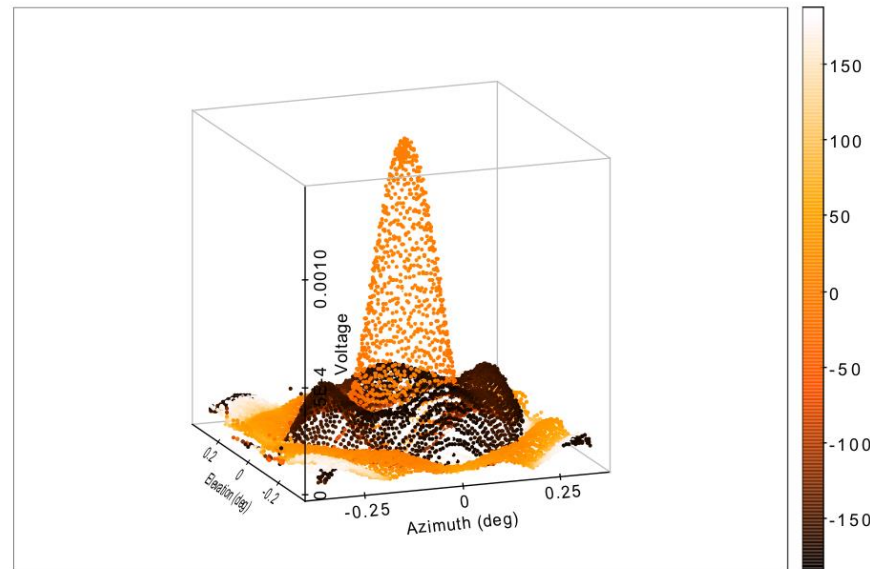


Image contrast (modulation) is highest at low spatial frequencies, decreasing to a value of zero as the spatial frequency increases $\rightarrow f(c)=D/\lambda$.

PSF set by detailed illumination pattern
(how it samples the aperture)



Point Spread Function (PSF)



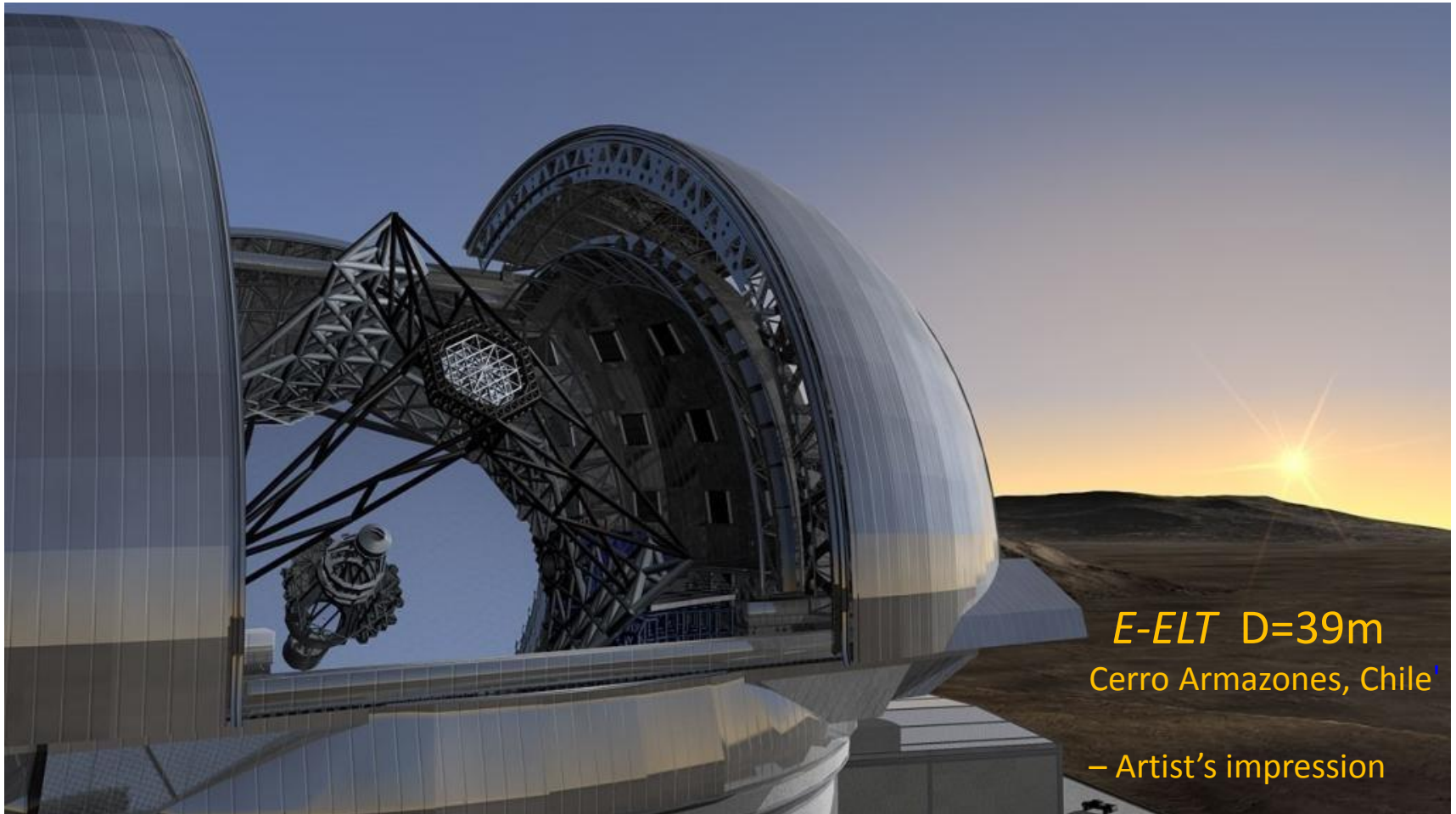
‘Shaped’
aperture
illumination
increases
aperture
efficiency at the
expense of PSF
near side-lobe
pattern

Apertures – Angular resolution & psf

A fully filled aperture (diffraction-limited refracting telescope)

Samples image spatial frequencies out to a cut-off set by objective diameter

But large optical telescopes are limited by 'seeing' – $D \sim 20\text{cm} \rightarrow \text{resolution} \sim 1''$



E-ELT $D=39\text{m}$
Cerro Armazones, Chile¹

– Artist's impression

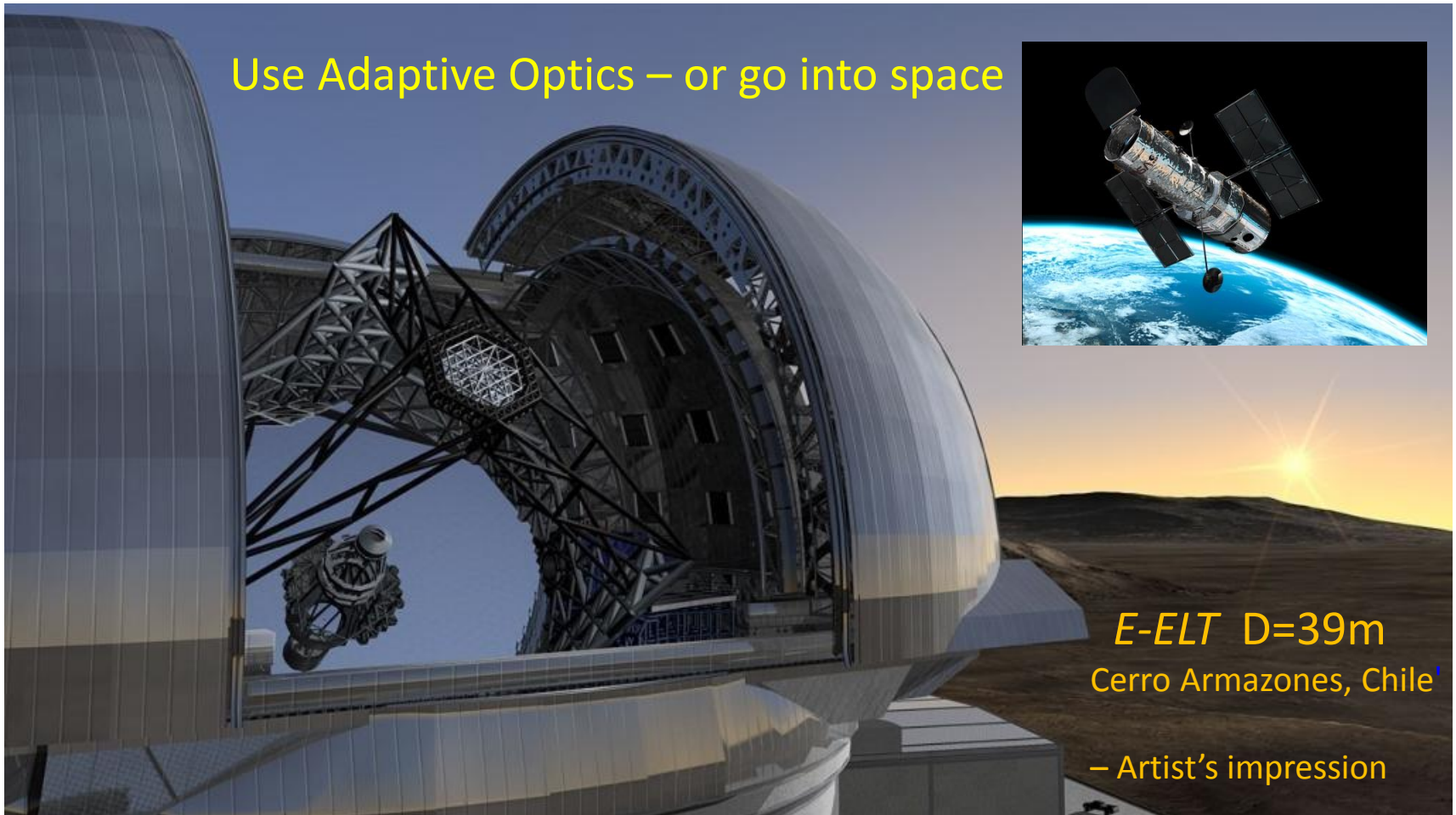
Apertures – Angular resolution & psf

A fully filled aperture (diffraction-limited refracting telescope)

Samples image spatial frequencies out to a cut-off set by objective diameter

But large optical telescopes are limited by 'seeing' – $D \sim 20\text{cm} \rightarrow \text{resolution} \sim 1''$

Use Adaptive Optics – or go into space



E-ELT $D=39\text{m}$
Cerro Armazones, Chile

– Artist's impression

Apertures – Sensitivity and Resolution

Large reflecting telescope

– Arecebo (d=300m)

Large steerable radio telescope

– Green Bank Telescope (d=100 x 110m)

Resolution = $\sim \text{wavelength} / \text{Diameter}$ (radians) \rightarrow few arcmins at centimeter λ
Excellent sensitivity from collecting area

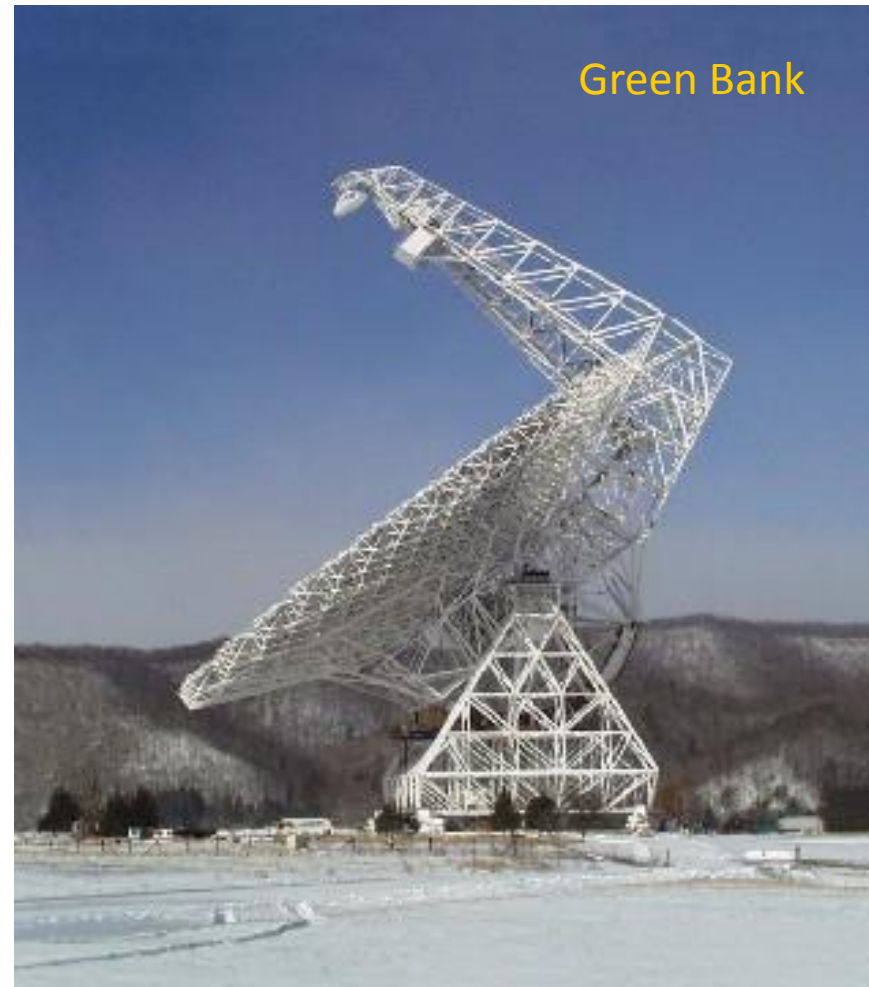
Optical telescope has resolution ~ 1 arcsec

At $\lambda=20\text{cm}$, need Diameter $\sim 35\text{km}$!

At $\lambda=3\text{mm}$, need Diameter $\sim 600\text{m}$



Arecibo



Green Bank

Apertures – Sensitivity and Resolution

Large reflecting telescope

– Arecebo (d=300m)

Large steerable radio telescope

– Green Bank Telescope (d=100 x 110m)

Resolution = $\sim \text{wavelength} / \text{Diameter}$ (radians) \rightarrow few arcmins at centimeter λ
Excellent sensitivity from collecting area

Optical telescope has resolution ~ 1 arcsec

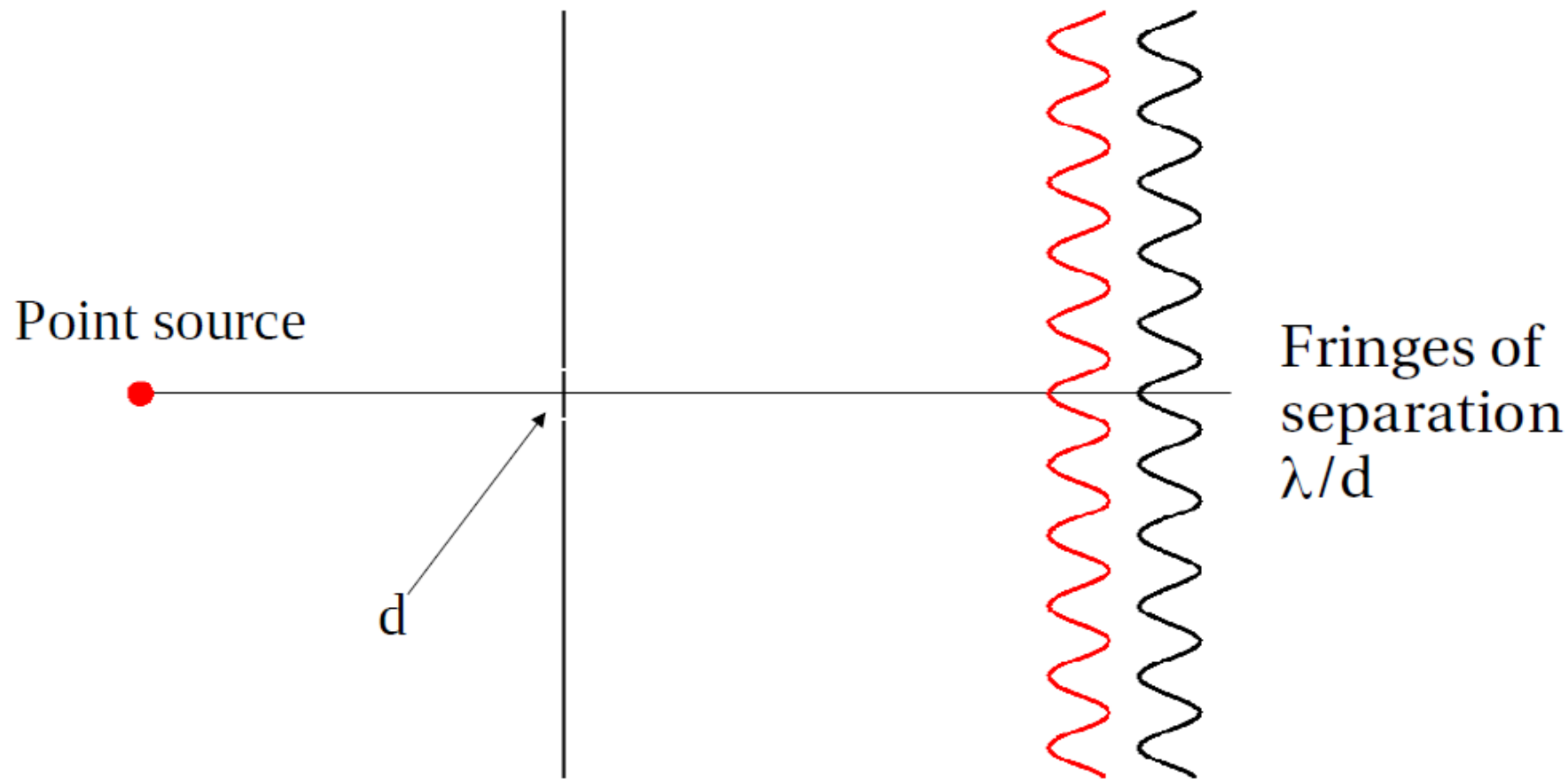
At $\lambda=20\text{cm}$, need Diameter $\sim 35\text{km}$!

\rightarrow Use an interferometer

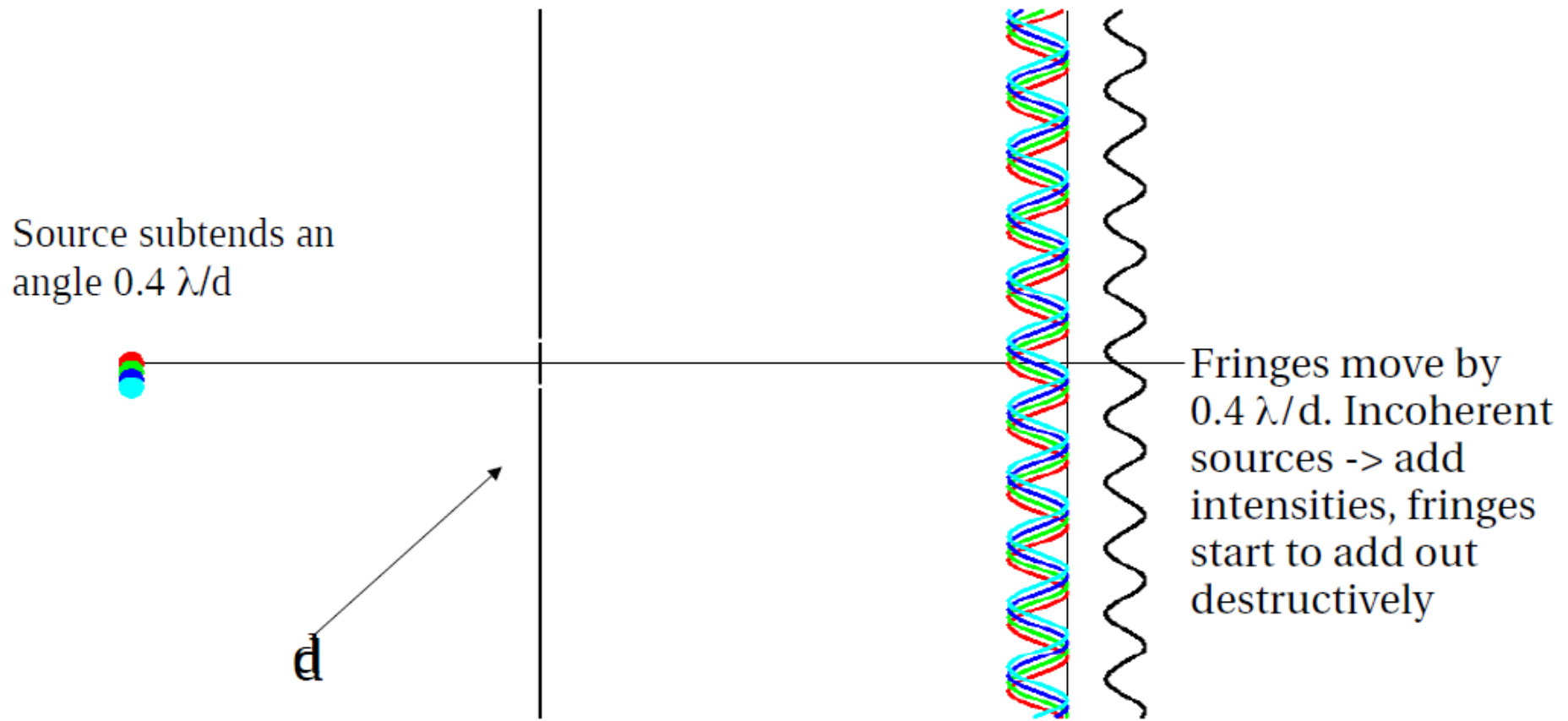
At $\lambda=3\text{mm}$, need Diameter $\sim 600\text{m}$



Young's slits revisited

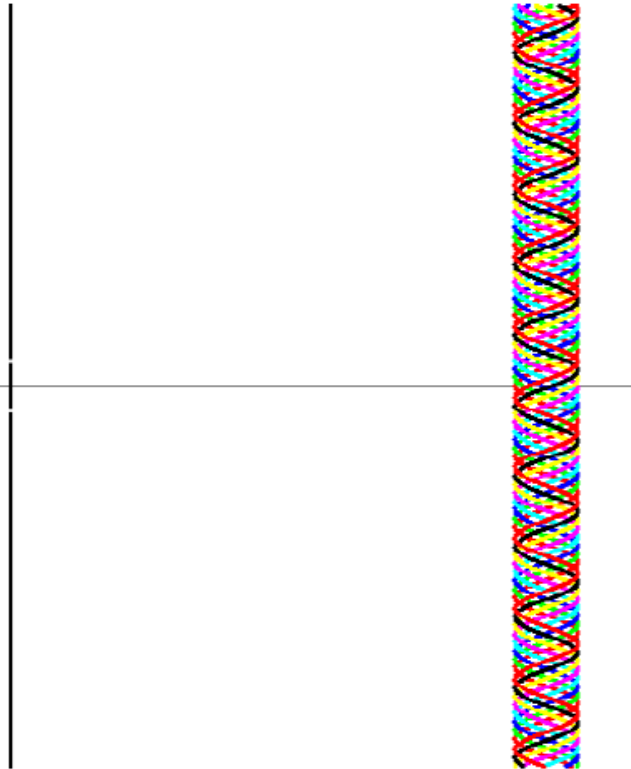


Larger source



Still larger source

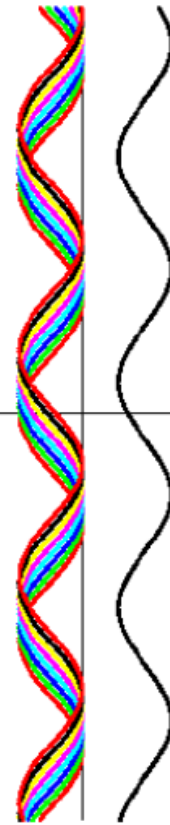
Source size
gets to λ/d



No fringes remain
(cancellation). Little
fringing seen for
larger sources than
 λ/d either.

Effect of slit size

Same size source,
but smaller slit

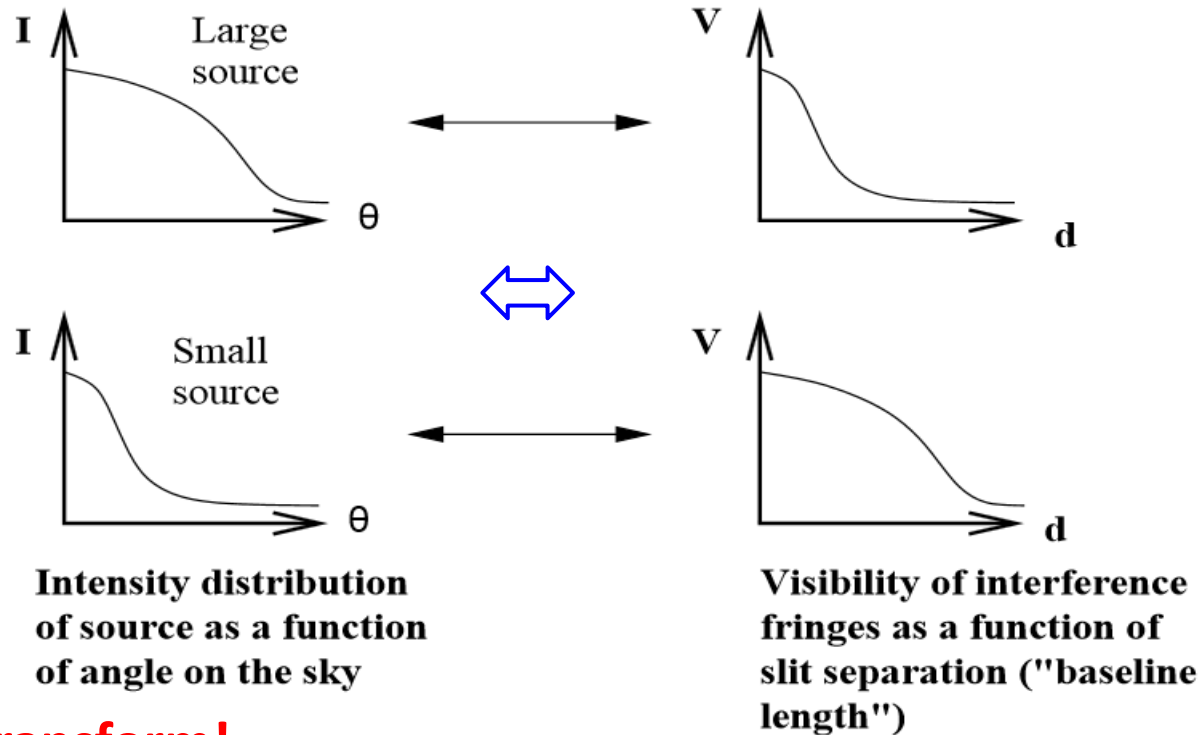


Increased fringe
spacing, so fringes
visible again

Young's slits: summary

Visibility of interference fringes $(V_{\max} - V_{\min}) / (V_{\max} + V_{\min})$

- Decreases with increasing source size ($V=1 \rightarrow$ unresolved point)
- Goes to zero when source size goes to λ/d
- For given source size, increases for decreasing separation
- For given source size and separation, increases with λ





It's a Fourier transform!

The fringe visibility of an interferometer gives information about the Fourier transform of the sky brightness distribution.

Long baselines record information about the small scale structure of the source but are INSENSITIVE to large-scale structure (fringes wash out)

Short baselines record information about large-scale structure of the source but are INSENSITIVE to small-scale structure (resolution limit)

Fringes

$$R(u, v) = e^{ik\mathbf{B.s}} \int I(x, y) e^{2\pi i(ux+vy)} dx dy$$


Fringe visibility $[R(u, v)]$

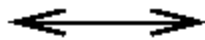
This is a series of **fast fringes** whose amplitude is the **Fourier transform of the source brightness distribution**

May need to get rid of fringes before integrating (fringe stopping).

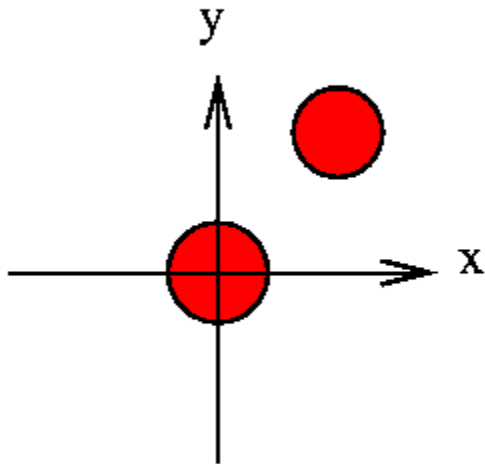
$R(u, v)$ has an amplitude and phase

The uv Plane

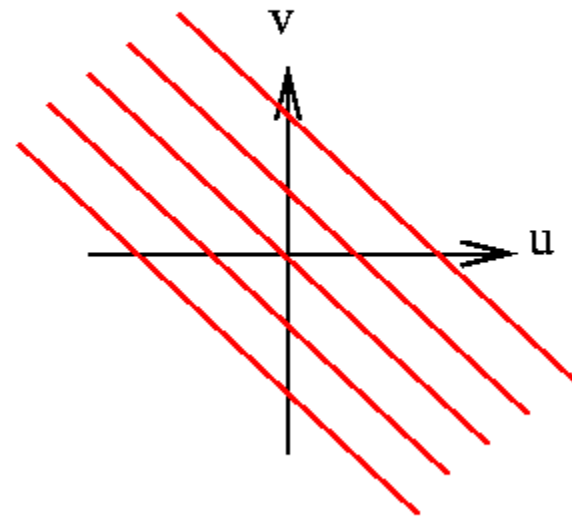
Source brightness as a function of angle



Fringe visibility as a function of baseline length in wavelengths



Double source of separation a arcsecond



Stripes of separation $206265/\lambda$ wavelengths

If we could measure Fringe Visibility for all u, v , \rightarrow Transform \rightarrow Image

Angular Resolution

20cm imaging (arcmin \rightarrow mas)

Allows astronomers to trace astronomical phenomena over orders of magnitudes in scale size



D=100m $\theta \sim 9.4'$



D=1km $\theta \sim 44''$



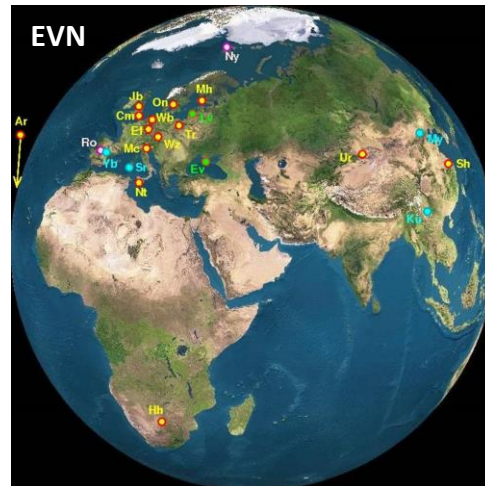
D=28km $\theta \sim 1.2''$



D=35km $\theta \sim 1''$



D=217 km $\theta \sim 150$ mas



D~10000 km $\theta \sim 5$ mas



$\theta \approx$ fraction of mas

Angular Resolution – Unfilled Apertures

Large number of antennas allow good snapshot capability

Allow Earth rotation to progressively populate the sampled aperture

Unfilled apertures do not sample all spatial frequencies present in the image
→ Limits the image quality & produces strong instrumental psf

Sampled spatial frequencies from the set of projected antenna spacings (in λ)

Large numbers of antennas + Earth rotation aperture synthesis

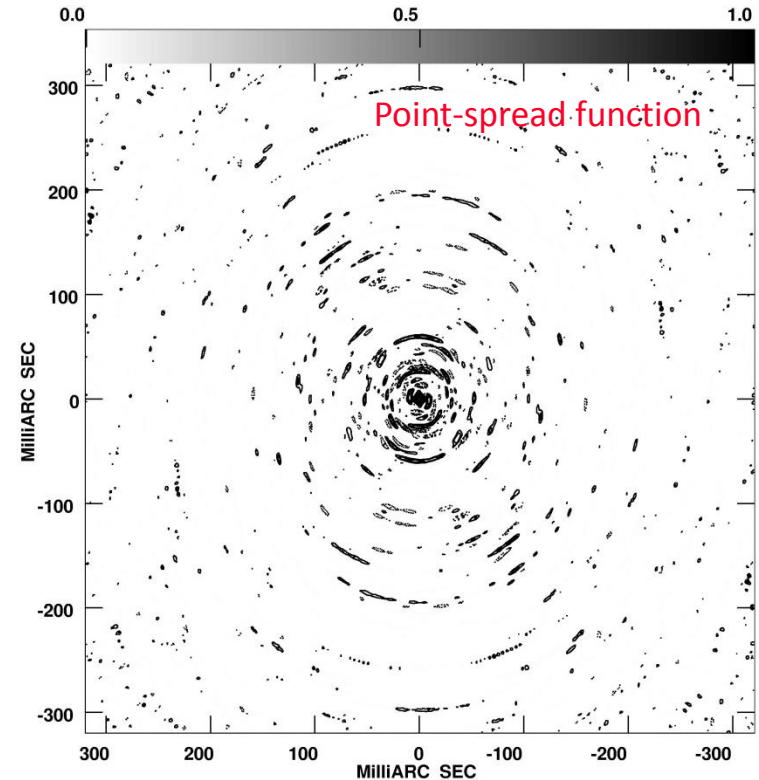
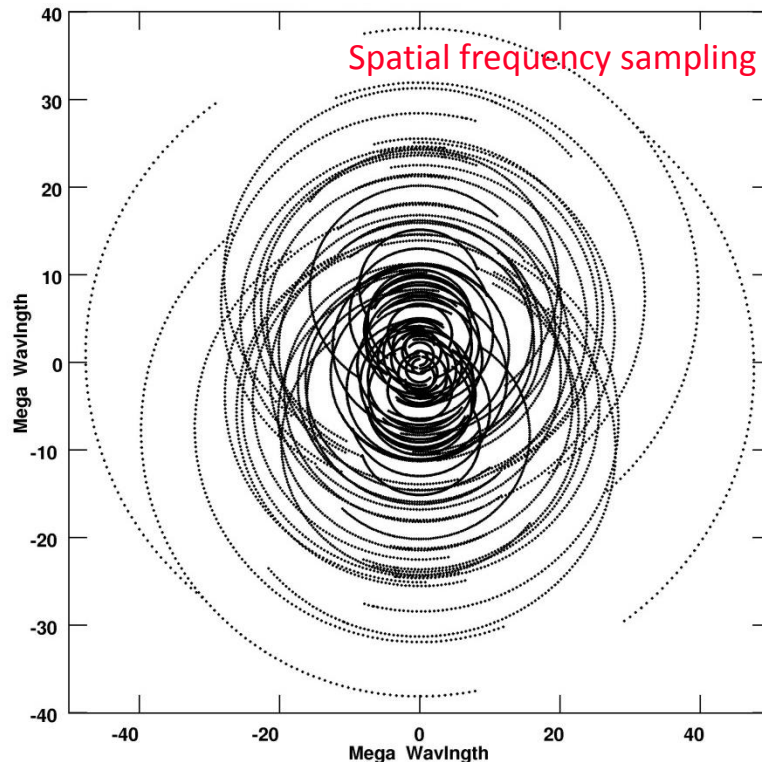
→ High quality images



Angular Resolution – Unfilled Apertures

Spatial frequency sampling \leftrightarrow point-spread function

Monochromatic 6-hr 10-element simulated observations

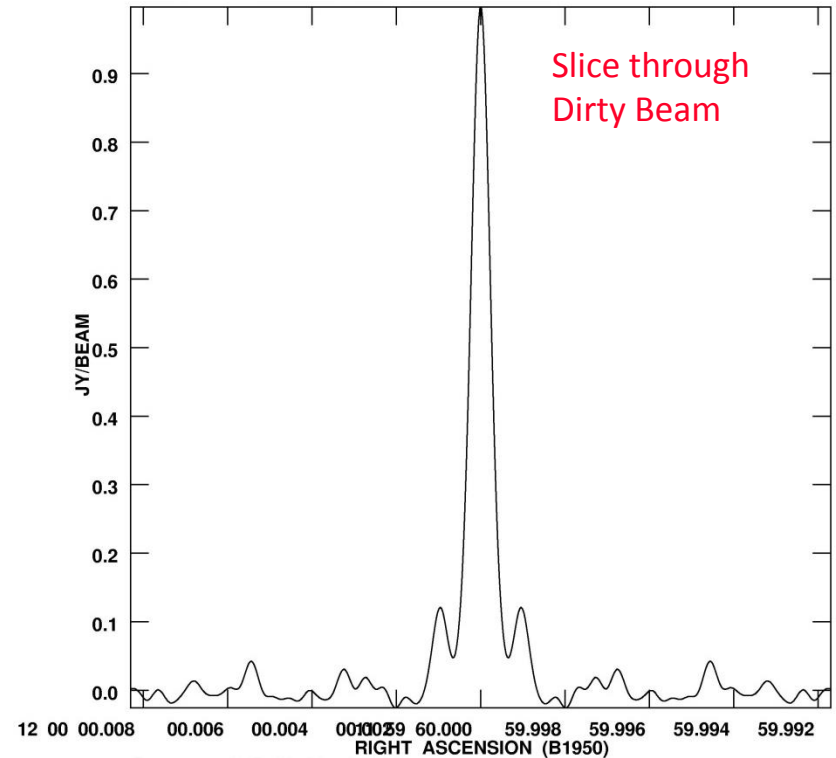
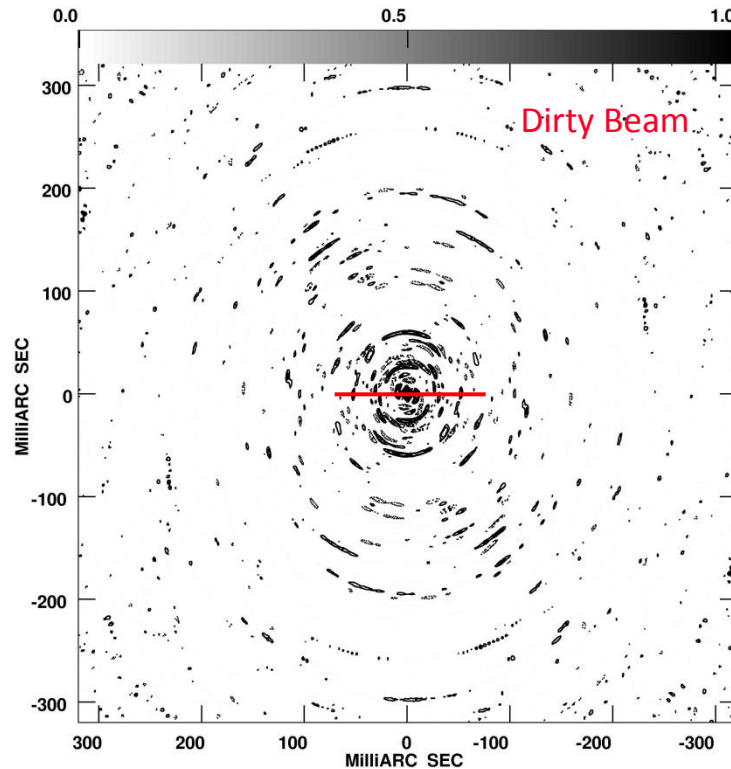


Holes in the spatial frequency sampling distribution produce a significant side-lobe response in the associated point spread function

Angular Resolution – Unfilled Apertures

Spatial frequency sampling \leftrightarrow point-spread function

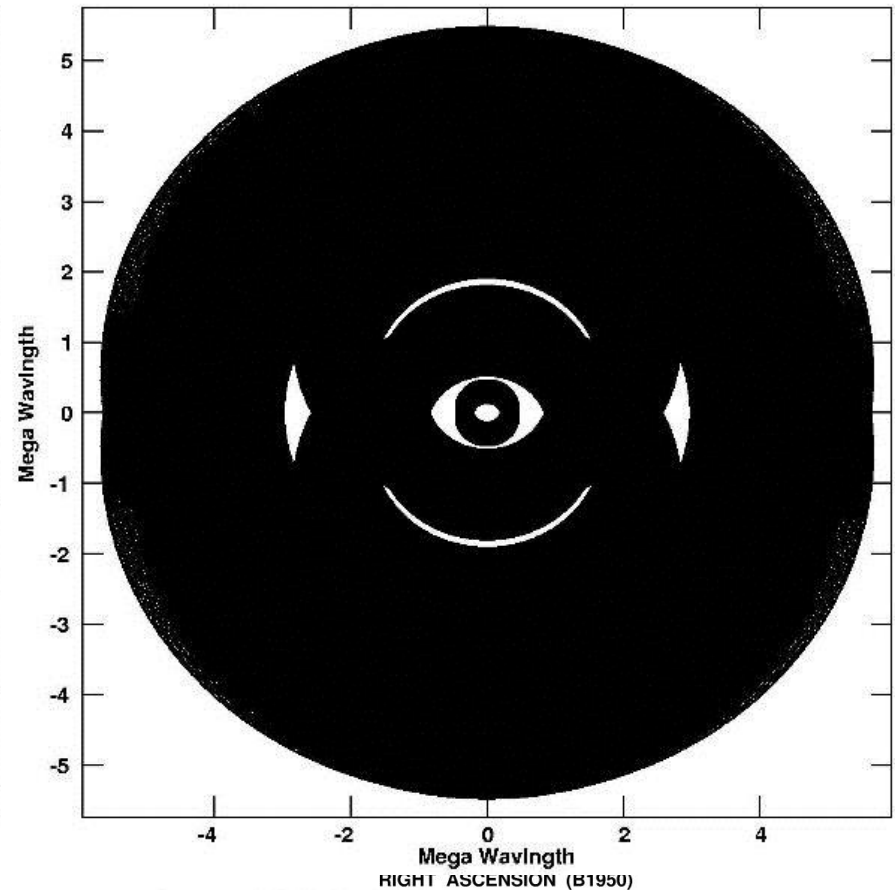
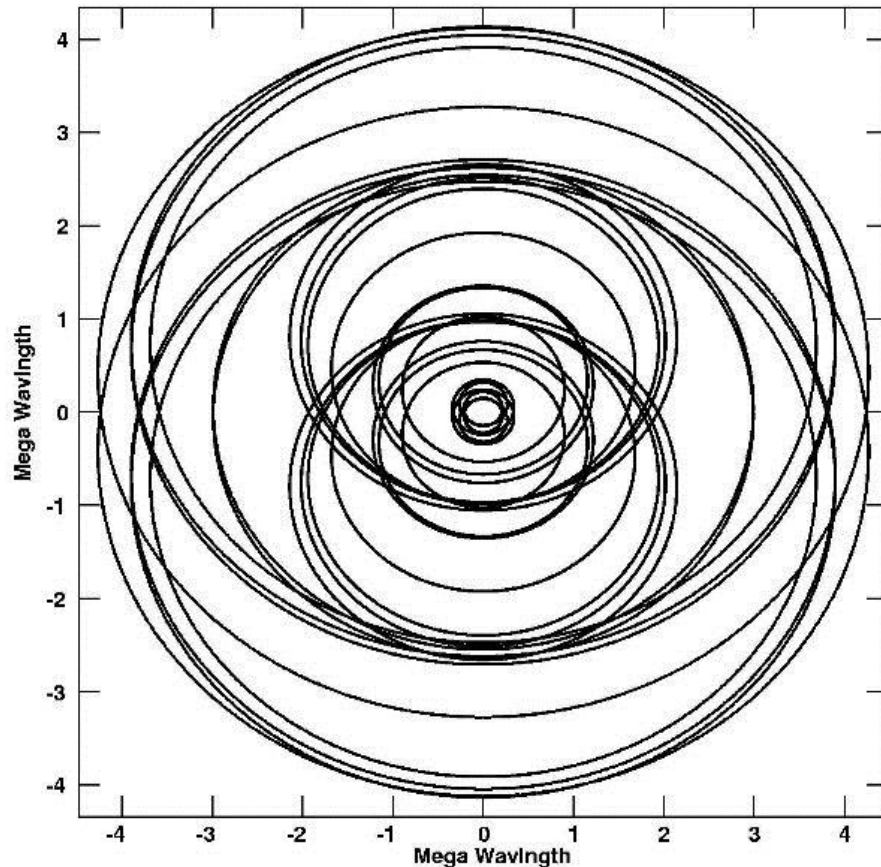
Monochromatic 6-hr 10-element simulated observations



Point-spread function (Dirty Beam) has complex side-lobe structure
Raw radio images require significant deconvolution of PSF to produce final images

Angular Resolution – Unfilled Apertures

Spatial frequency sampling \leftrightarrow point-spread function



Point-spread function and image fidelity can be improved by increasing the bandwidth of the observations \rightarrow partially filled aperture – also improves sensitivity
Multi-Frequency Synthesis (MFS) \rightarrow need to account for image spectral variation

Angular Resolution – Unfilled Apertures – ALMA

Aperture synthesis array optimised for wavelengths of 1cm–0.3mm (30–950 GHz)

High, dry site, Chajnantor Plateau, Chile (5000m)

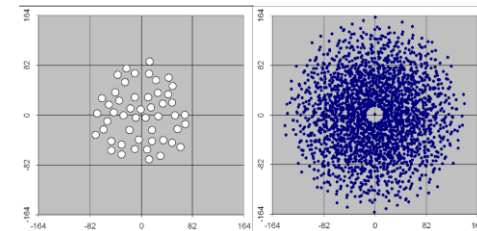
54 12m (main array)
+ 12 7m antennas (ALMA compact array - ACA)



Low fractional bandwidth – but....
Excellent snapshot capability with 54 antennas
Earth rotation improves aperture coverage

Baselines from ~15m to 16km – **Resolution**/arcsec $\sim 0.2(\lambda/\text{mm})/(\text{max baseline}/\text{km})$
5 mas for highest frequency/longest baseline

Sensitive, wide-band (8 GHz) receivers; full polarization
Flexible digital correlator giving wide range of spectral resolutions.



Initial Calibration: RFI Excision (in cm bands)

– New broad-band interferometers operate well outside protected bands!!

Lower frequency observing bands tend to suffer more RFI problems

Many software packages have interactive RFI excision – but time consuming!!

Automatic scripting is being developed – after initial template flagging - *known RFI*

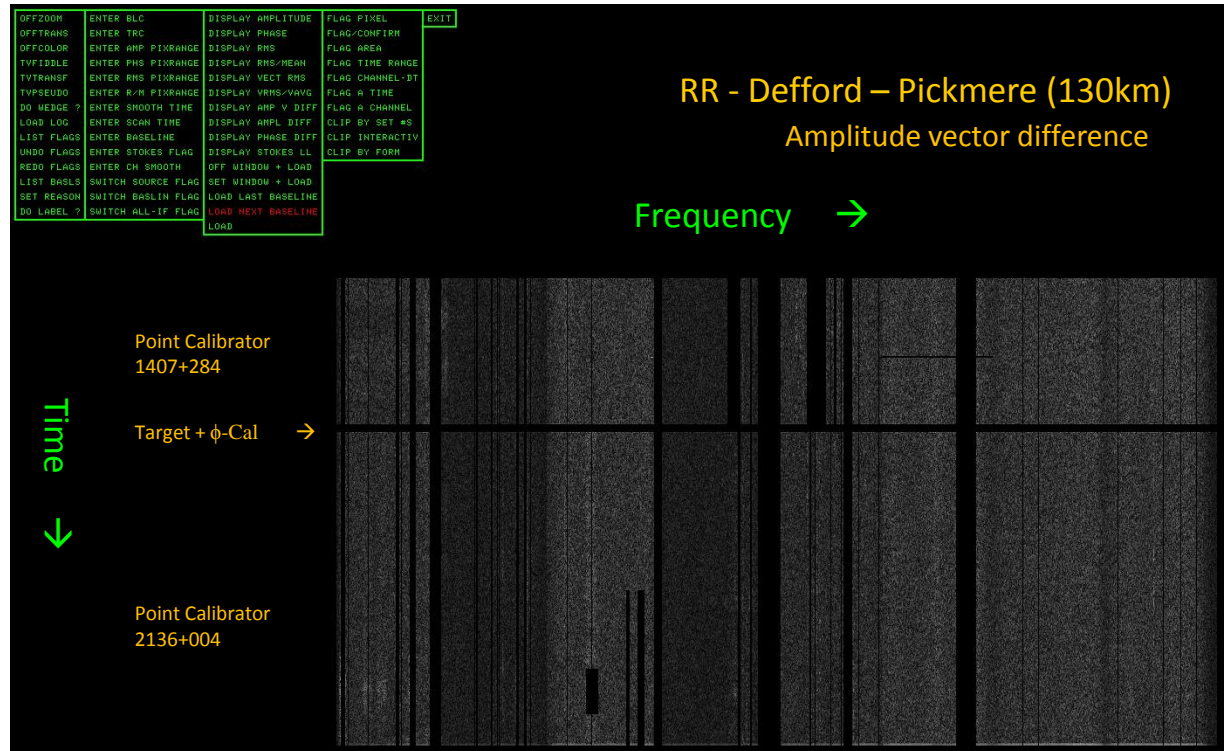
e-Merlin L-Band (8x64MHz IFs):

512MHz (1254 – 1766 MHz) BW

512 x 125kHz channels per IF

Large RX headroom ensures
linearity (+ 8-bit digitisation)

Typically only lose 10-15% of
total passband



Initial Calibration: Delay Correction

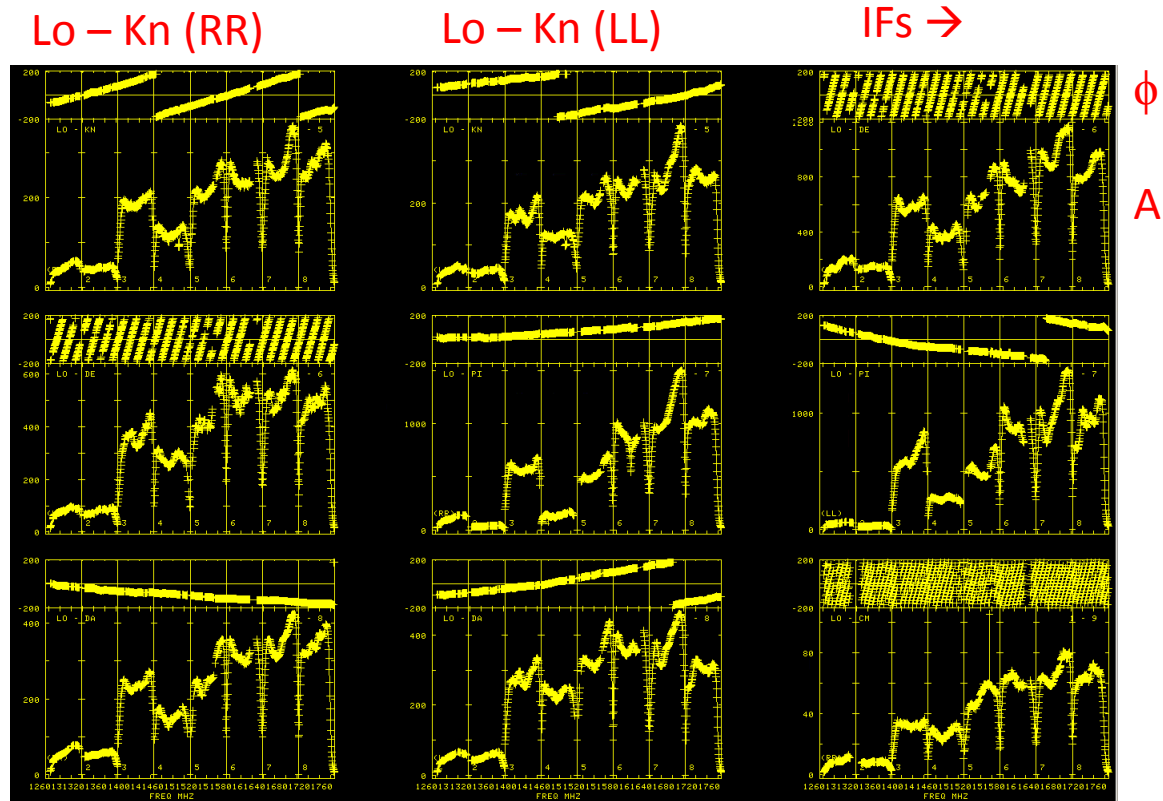
Not geometric (Earth rotation) – delay applied by correlator in real time
– data transport delays / electronic delays from distant antennas

Wide-band data from many telescopes delivered with delay correction applied

Some instruments (EVN, *e*-Merlin....) require delay corrections to be calculated at an early stage of data reduction – using sources with good s:n (usually calibrators)

Multi-IF spectral plots of raw data will show delay errors from phase slopes across the pass-band

Single or multi-IF delays can be found (usually multi-IF unless you expect different delays for each IF)



Initial Calibration: Delay Correction

Wide-band data from many telescopes delivered with delay correction applied

Some instruments (EVN, *e*-Merlin....) require delay corrections to be calculated at an early stage of data reduction – using sources with good s:n (usually calibrators)

Use unaveraged data for accurate large delay solutions
→ data are Nyquist sampled

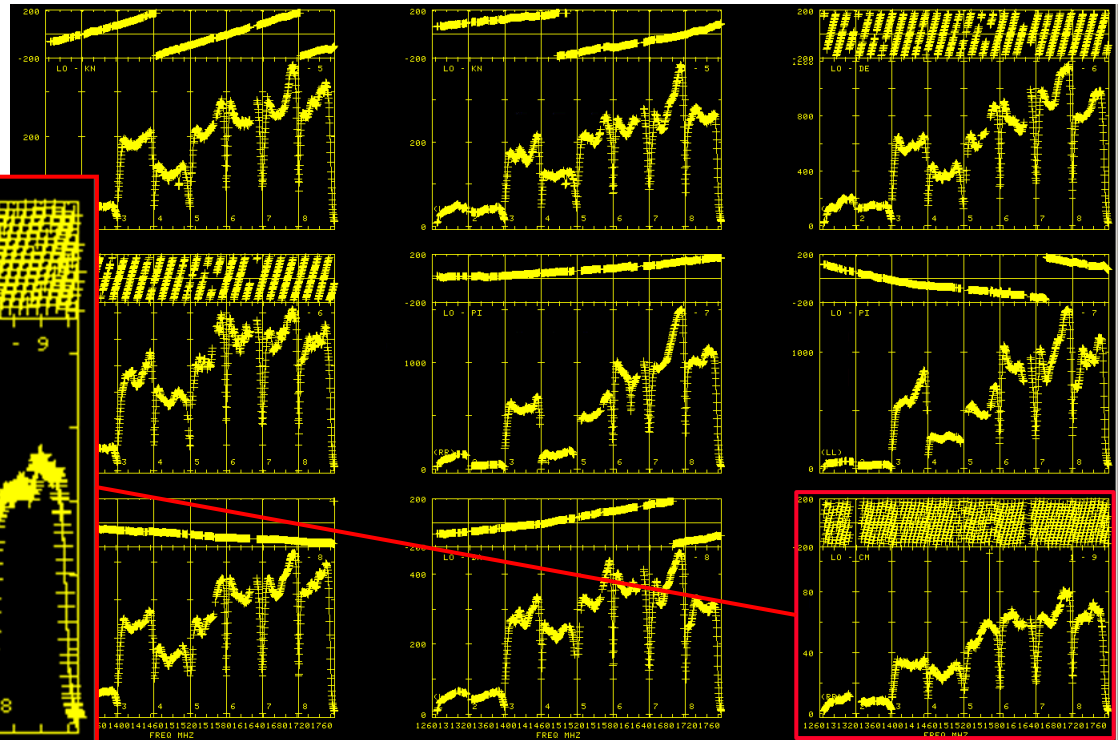
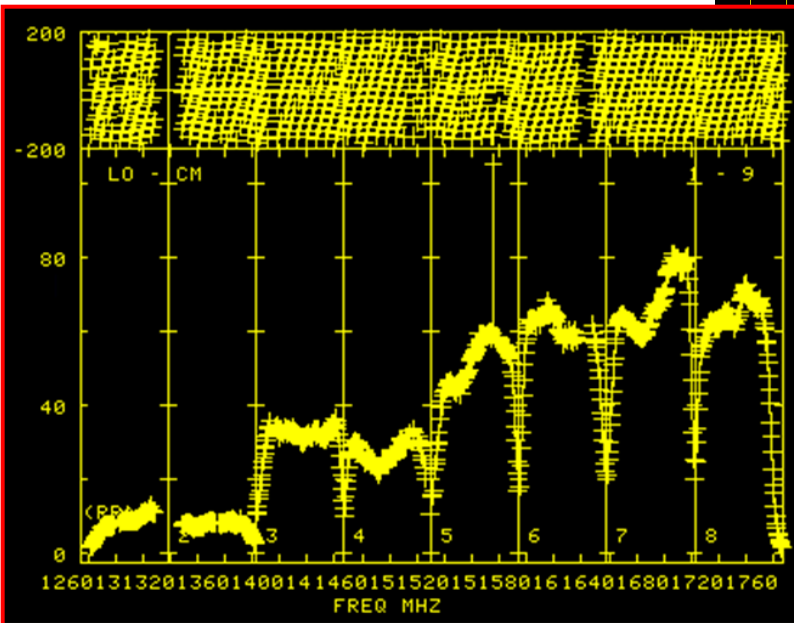
Lo – Kn (RR)

Lo – Kn (LL)

IFs →

ϕ

A



Initial Calibration: Gain Calibration

Point source primary calibrators – variable (t ~days - months)

Flux density primary calibrator – not variable but resolved (modelled)

Phase calibrator (secondary) – observed often (near point-like)

Amplitude scale usually set by primary and flux density calibrators

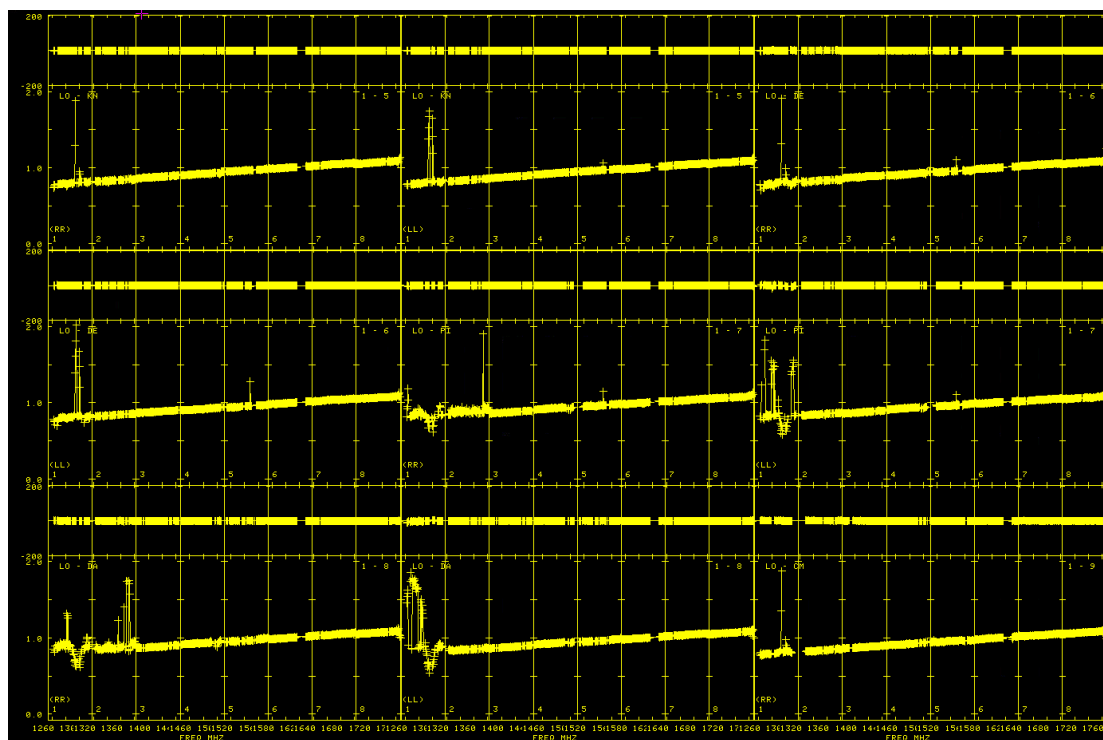
Phases (& gain tweaks) for target from phase-calibrator (8:2 min cycle)

Final fine adjustments made through band-pass calibration (bright calibrators only) to flatten the IF responses

Corrected data on 1407+284 after final delay, phase, gain, and bandpass corrections

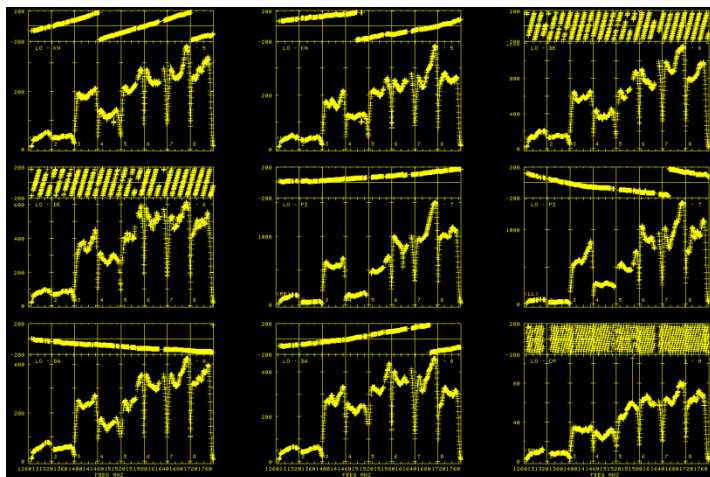
1407+284 is a point source with a rising spectrum

Some RFI still present - IFs 1&2



Point calibrator 1407+284

Initial Calibration: Gain Calibration



← Before

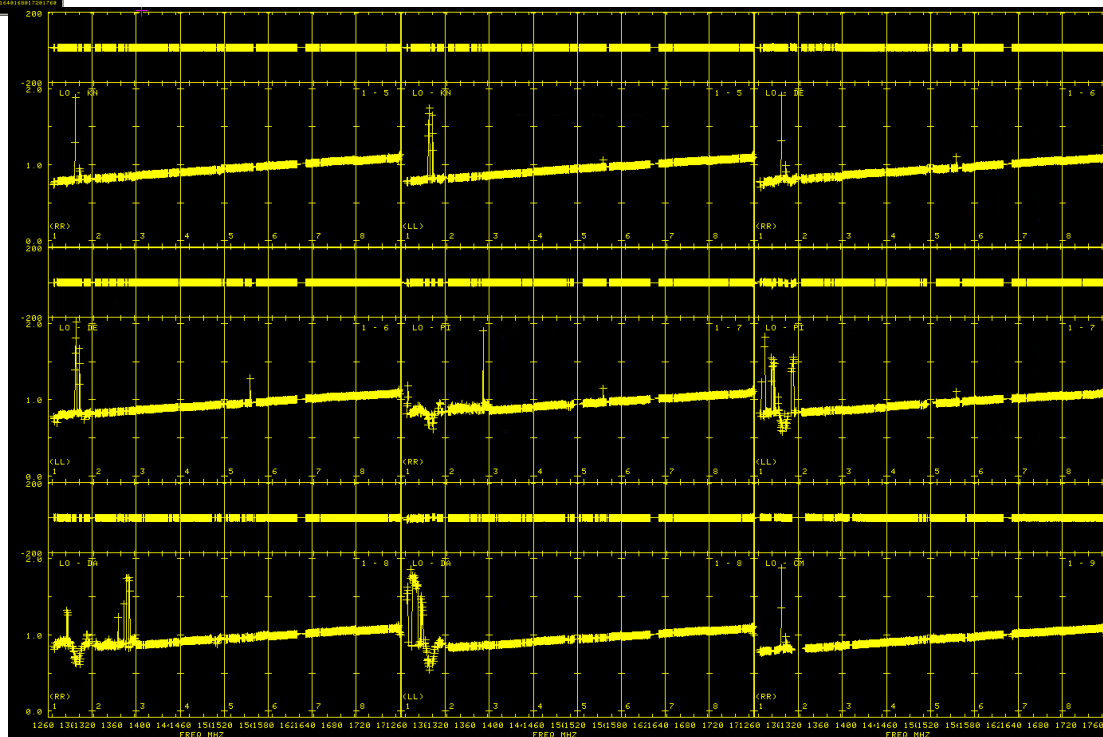
After ↓

Final fine adjustments made through band-pass calibration (bright calibrators only) to flatten the IF responses

Corrected data on 1407+284 after final delay, phase, gain, and bandpass corrections

1407+284 is a point source with a rising spectrum

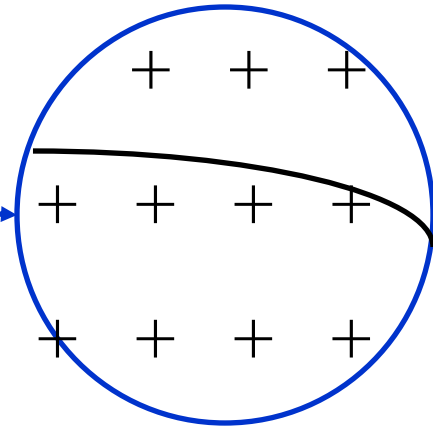
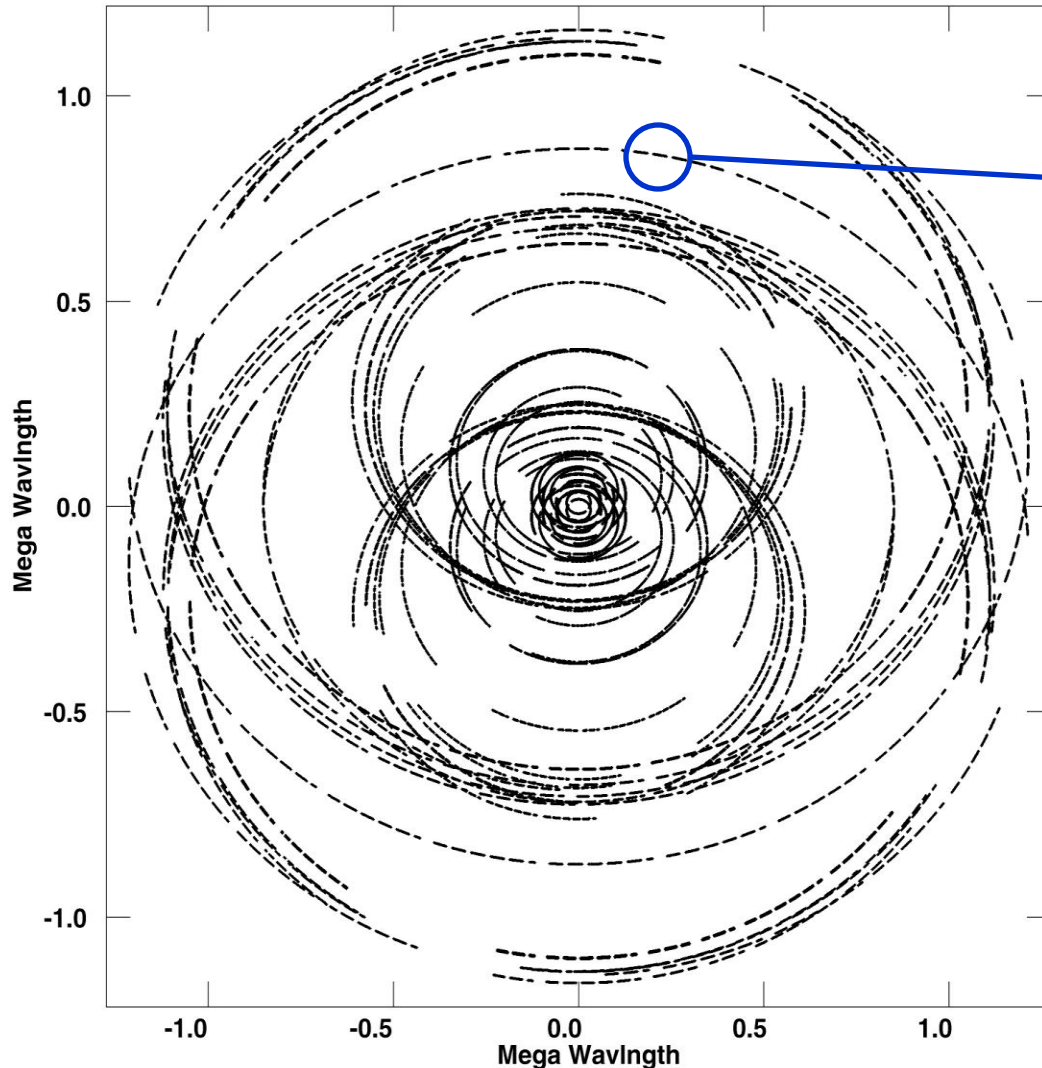
Some RFI still present - IFs 1&2



Point calibrator 1407+284

Imaging: Data Gridding – 1

Integrations are distributed over a greater number of sampled grid points in the outer u - v plane than in the inner regions

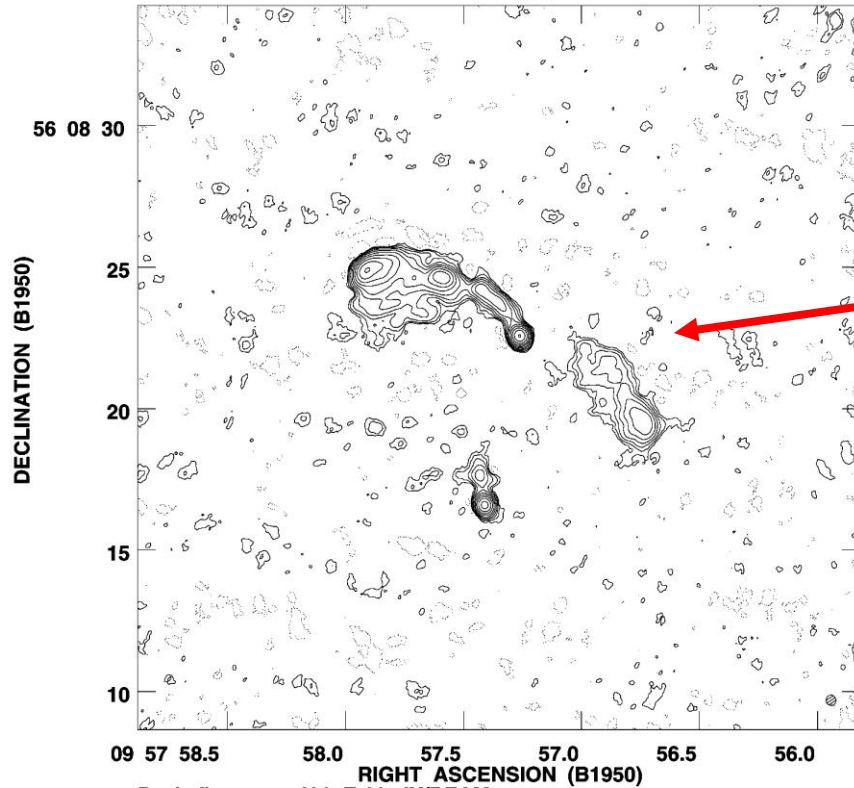


Data are interpolated onto a regular 2^n grid with a spheroidal convolution function

Weights unmodified by local density – 'Natural' weighting

Weights divided by local density of points – 'Uniform' weighting

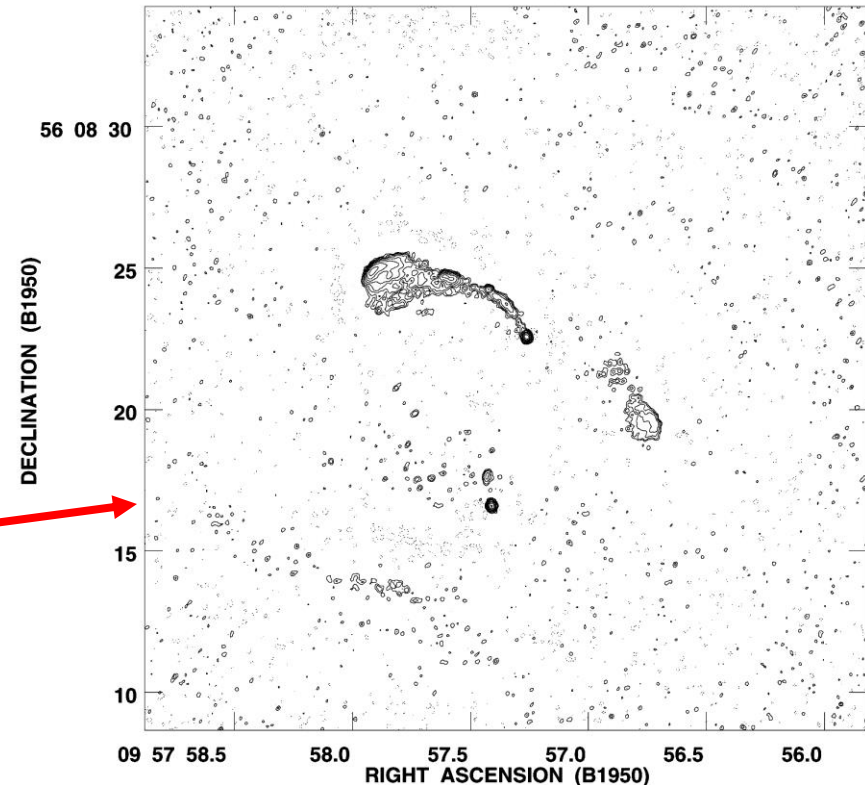
Imaging: Data Gridding – 2



Naturally weighted images will give better sensitivity at the expense of angular resolution – low spatial frequencies are weighted up & data are utilised optimally

Uniformly weighted images will give better angular resolution at the expense of sensitivity – low spatial frequencies are weighted down and the data are not utilised optimally

– may be subject to a striping instability

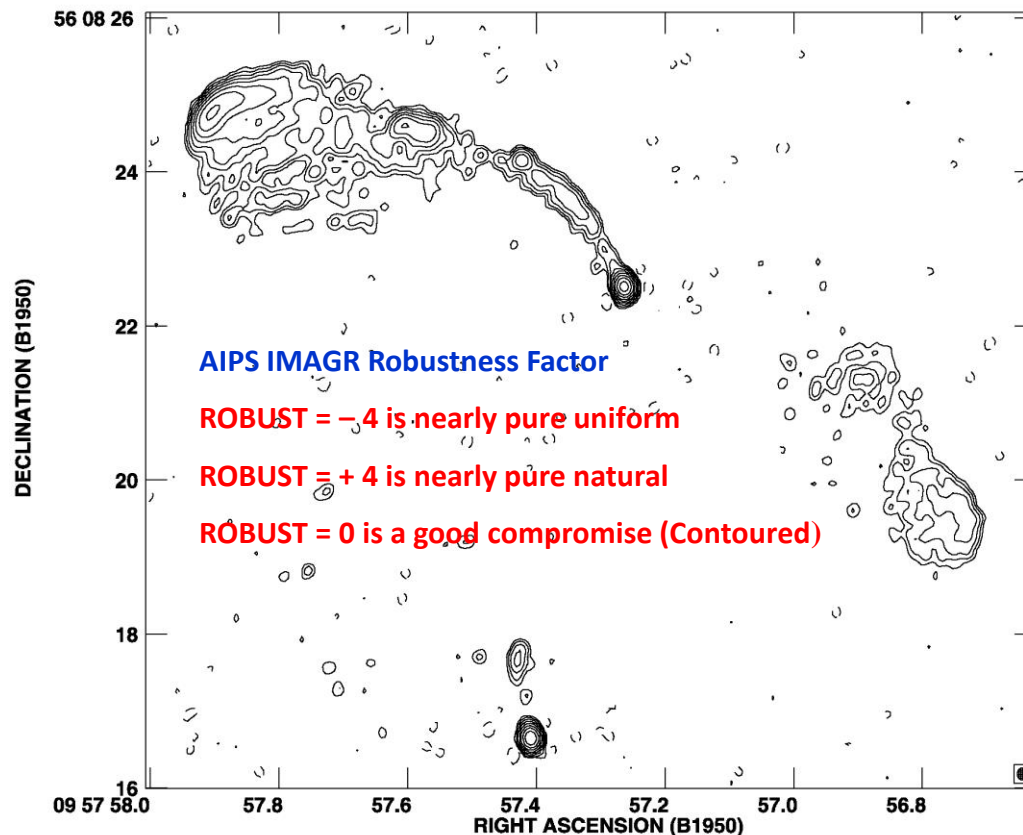


Imaging: Data Gridding – Robustness

Originally derived as a cure for striping instability

– Natural weighting is immune and therefore most ‘robust’

Robustness varies effective weighting as a function of local u - v weight density

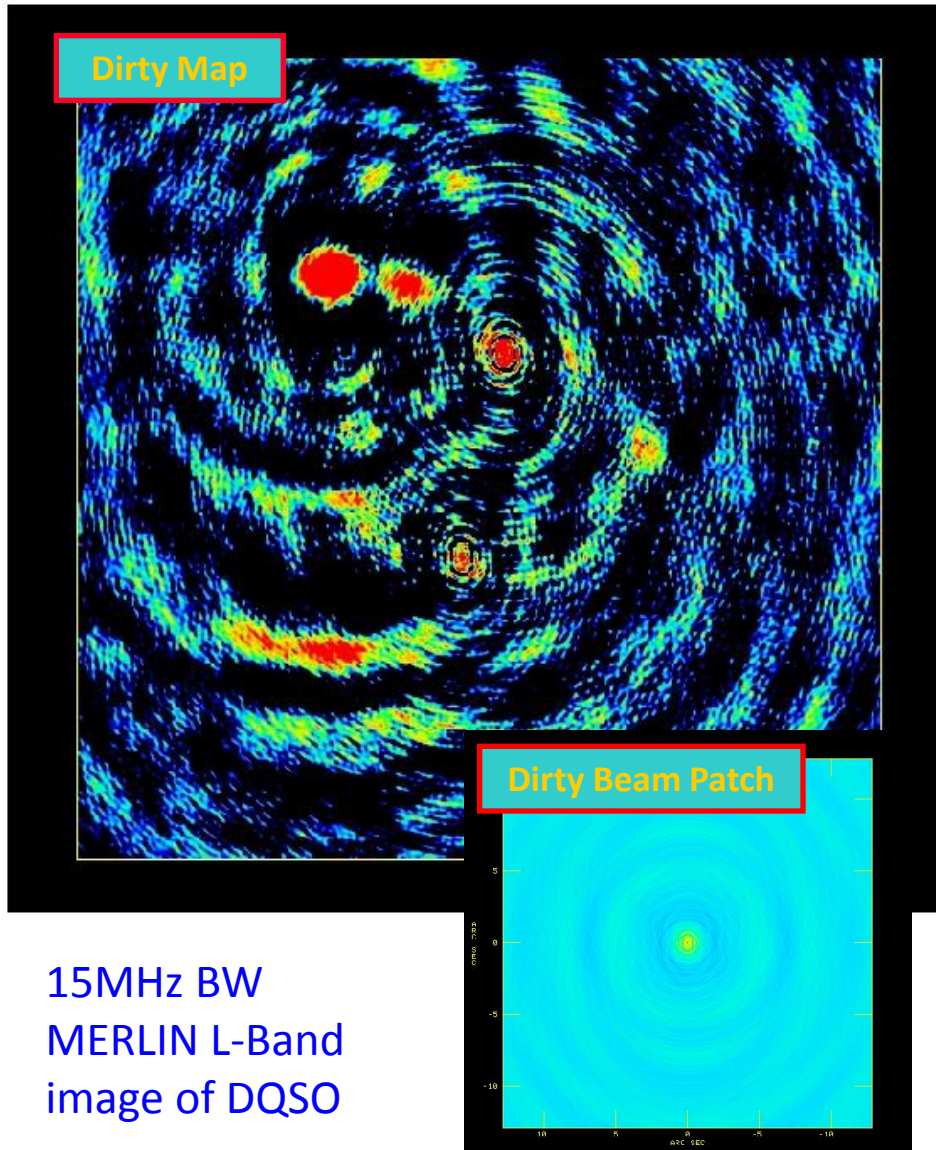


Modifies the variations in effective weight found in uniform weighting → more efficient use of data & lower thermal noise

Selecting a mid-range robustness factor can produce images close to uniform weighting resolution with noise levels close to naturally-weighted images

Imaging: Deconvolution

Unsamped regions in the telescope aperture give rise to severe ripples in the beam (psf)



The raw Fourier-transformed image (dirty map) will usually require significant deconvolution. Beam patch centred under brightest image feature and a patch scaled by ~ 0.1 subtracted. (Minor cycle)

Beam patches which are then Fourier transformed back to the data plane and (vector) subtracted before re-gridding and transforming to form a new residual image (Major Cycle)

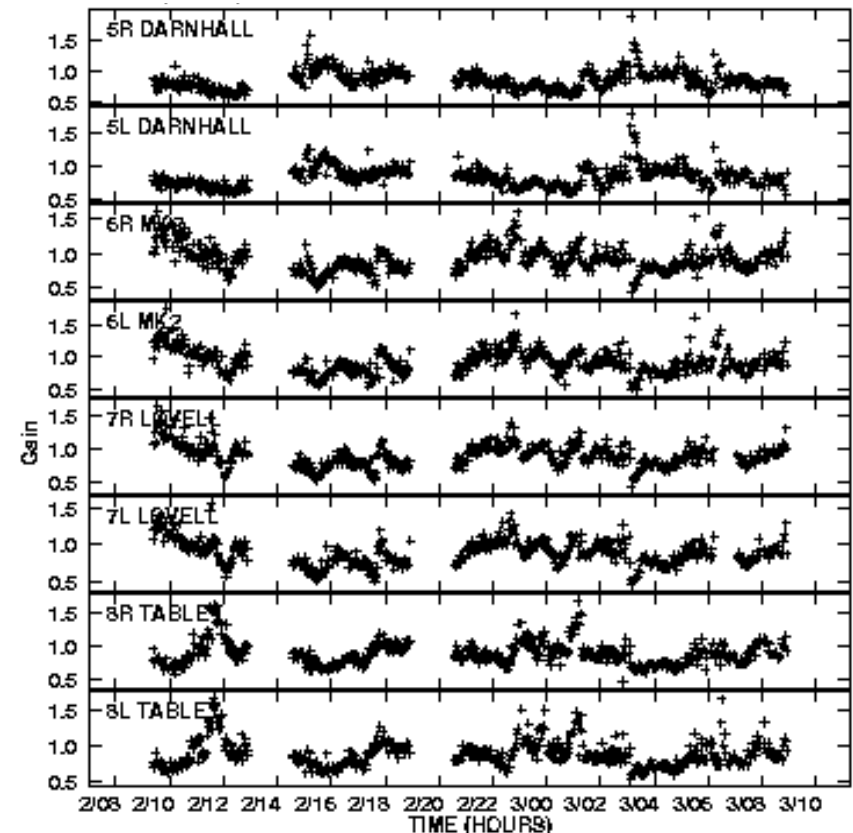
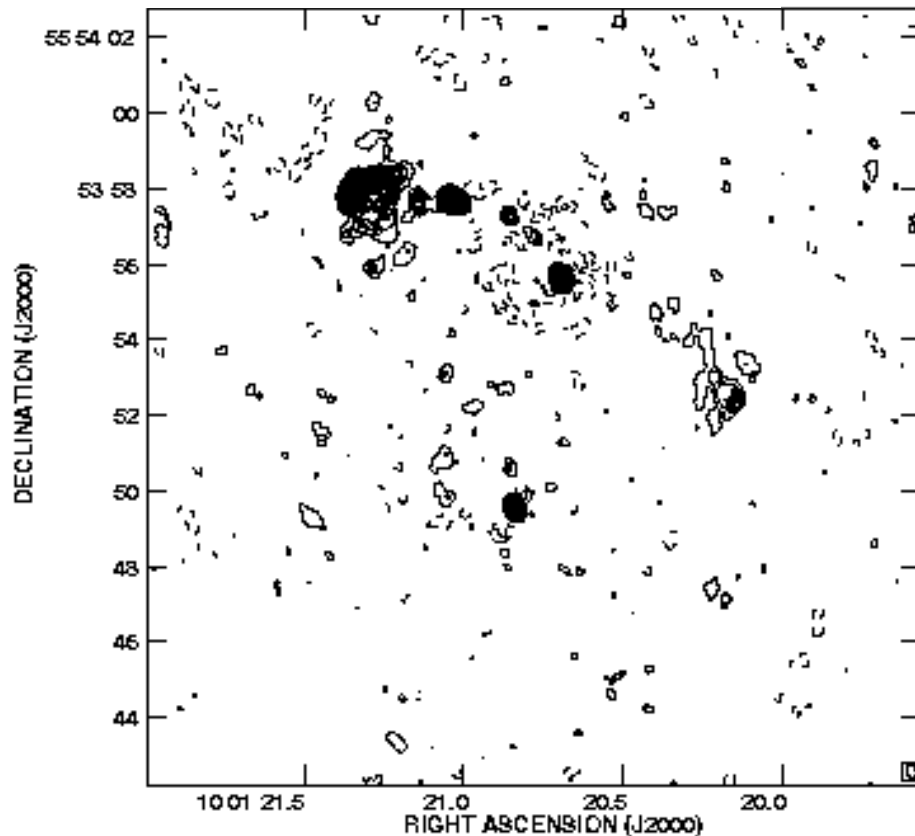
Continue until residual map shows thermal noise

Add back to final residual image idealised clean beams fitted to central part of dirty beam at each subtraction point

Secondary Calibration: Self-Calibration

Image and deconvolve target source after applying initial phase & gain solutions

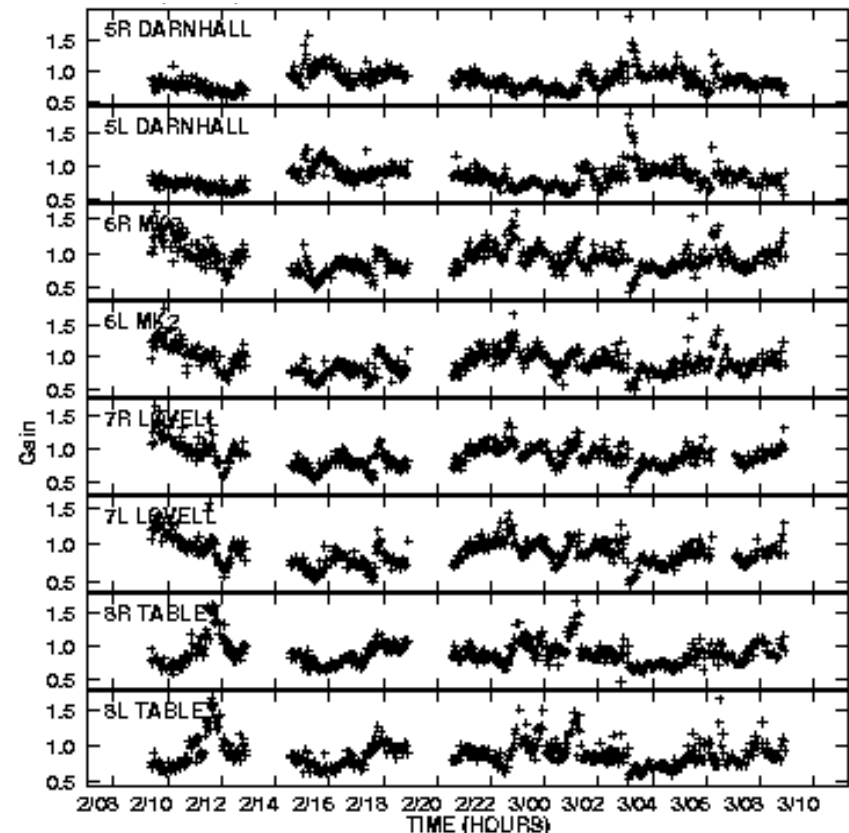
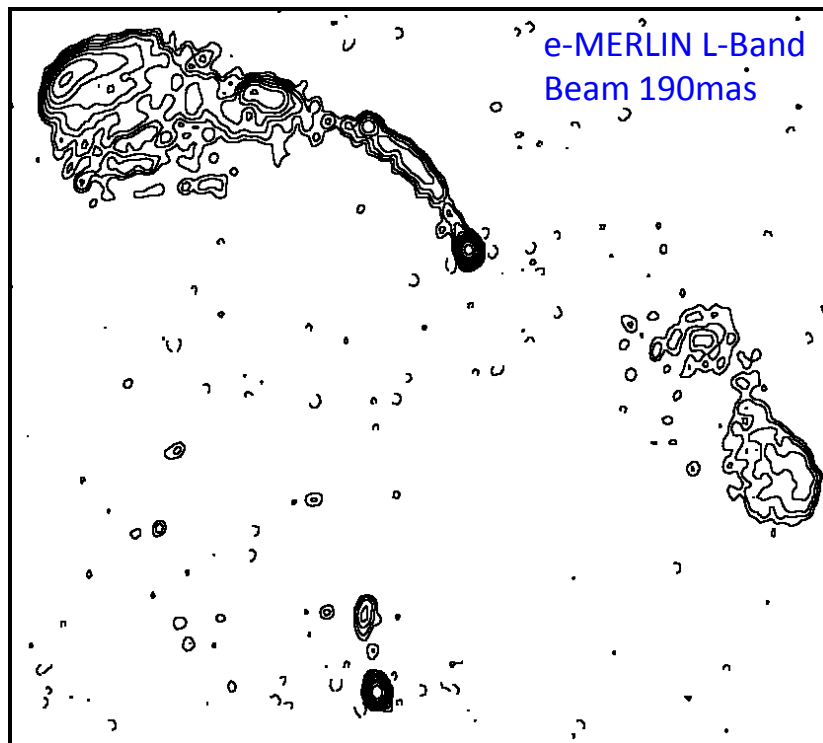
If target is bright enough, use the initial target image to apply further self-calibration refinements to the phase and gain solutions → sharpens image in situ

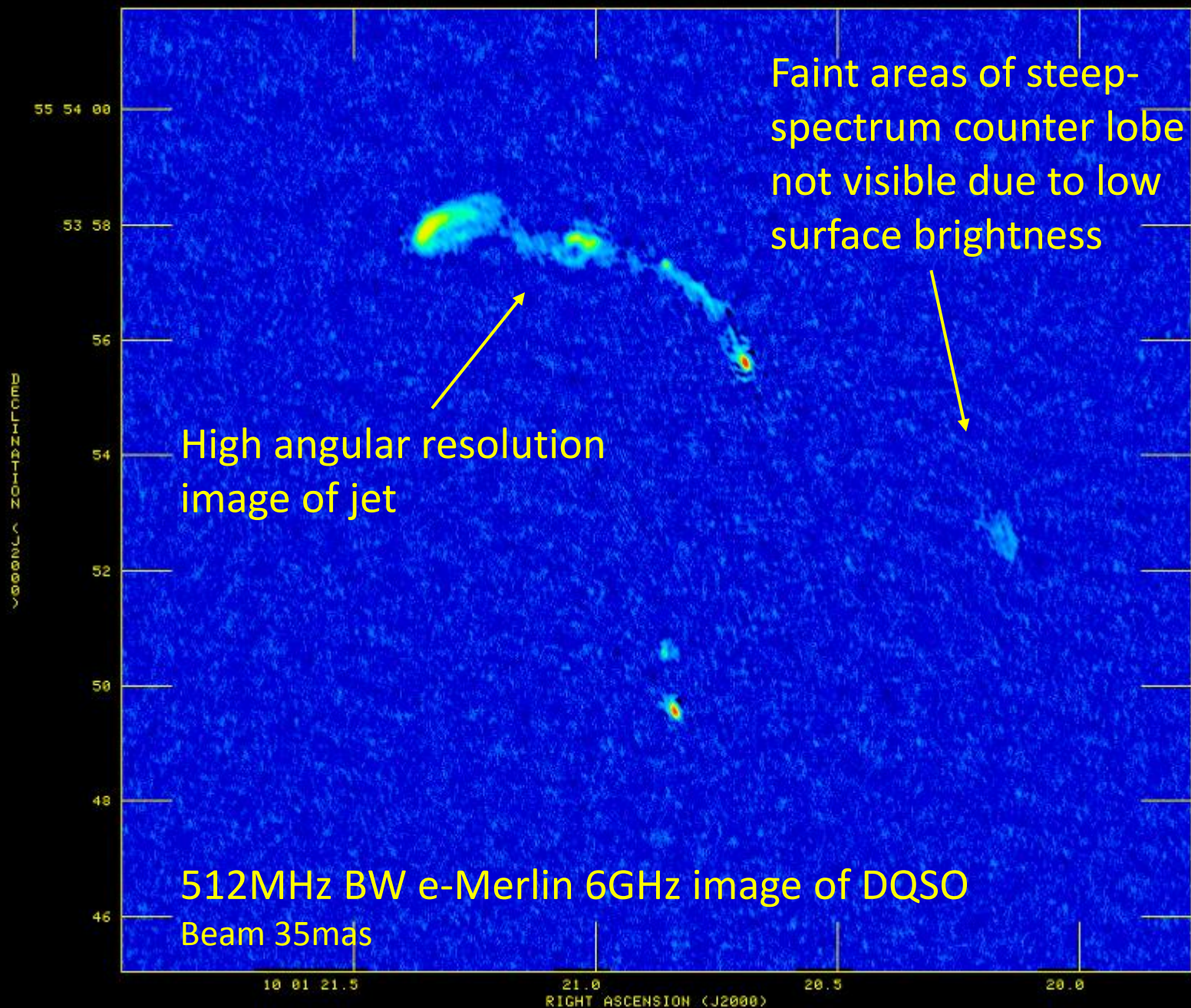


Secondary Calibration: Self-Calibration

Image and deconvolve target source after applying initial phase & gain solutions

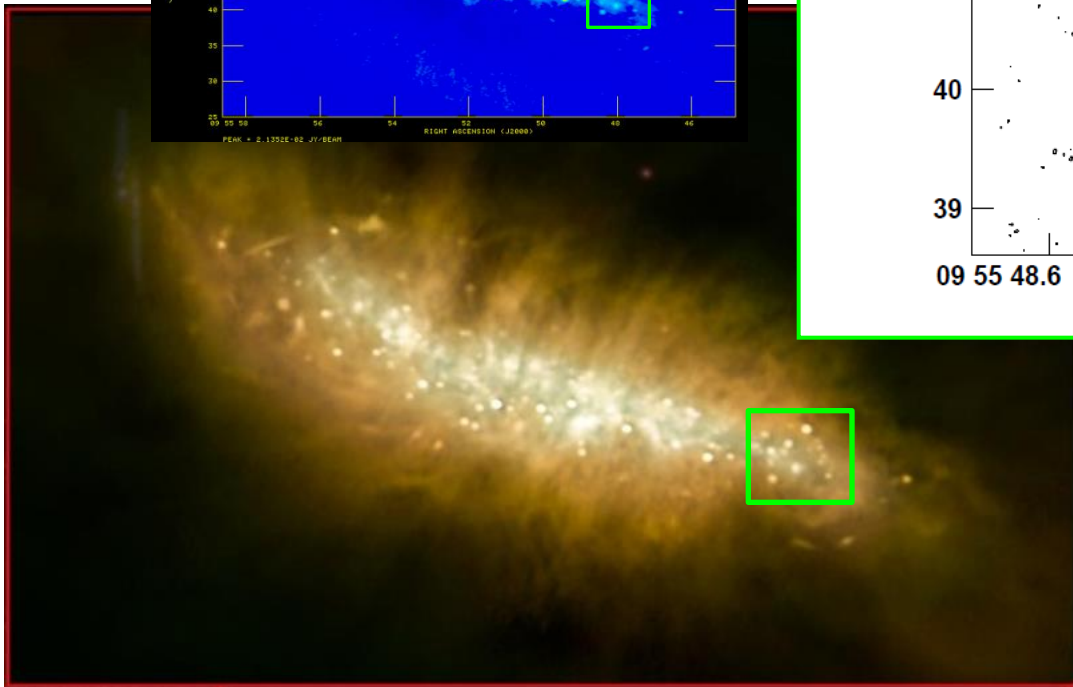
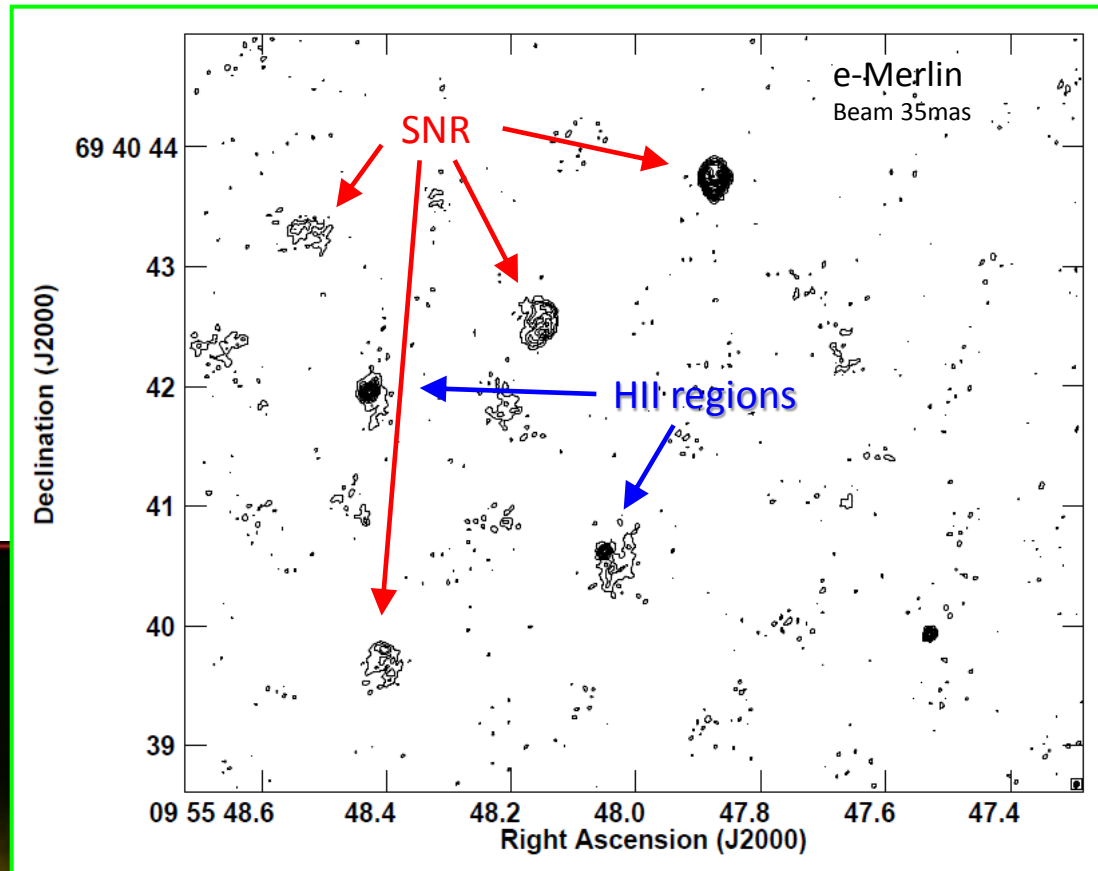
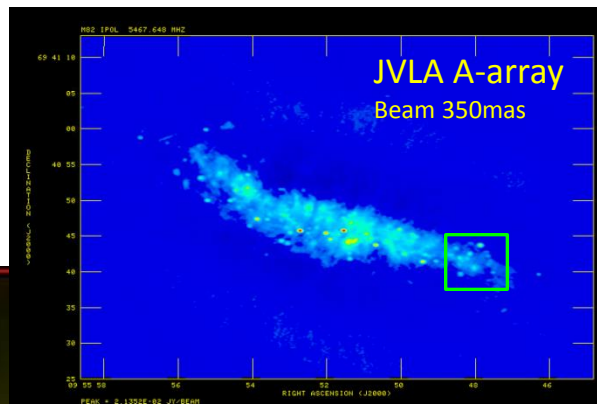
If target is bright enough, use the initial target image to apply further self-calibration refinements to the phase and gain solutions → sharpens image in situ





Spatial Frequency Content and Surface Brightness

JVLA & e-Merlin 5GHz images of M82



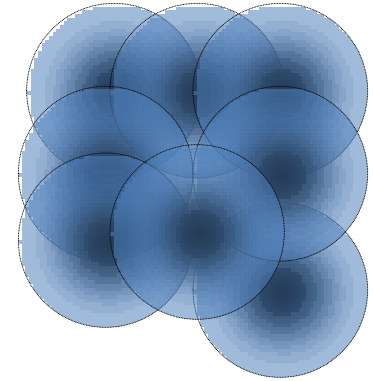
JVLA C-Band image of M82 (A+B array) with the section imaged at high resolution above marked in green.
After Marvil, Owen, and Eilek

Wide-Field Imaging

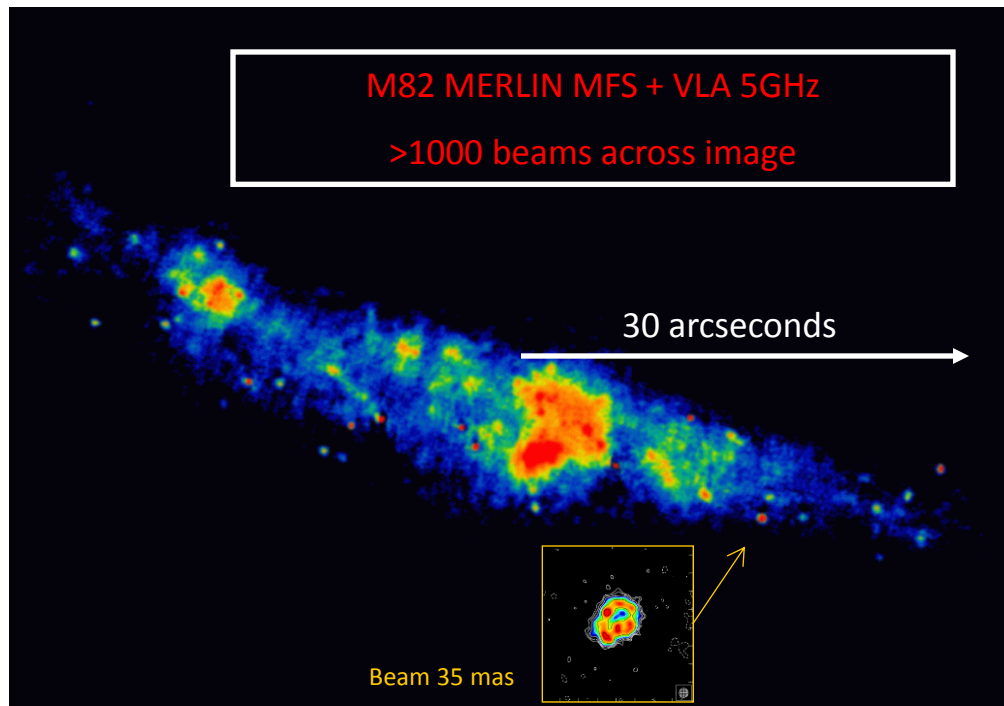
Images with large numbers of resolution elements

Imaging across the interferometer primary beam

– or mosaicing across several primary beams...



- Alleviated by observing lots of narrow channel bandwidths & short integration times
- Not usually a major problem for ALMA with small primary beams....



Wide-field images are subject to a number of possible distortions:

Non-coplanar baselines

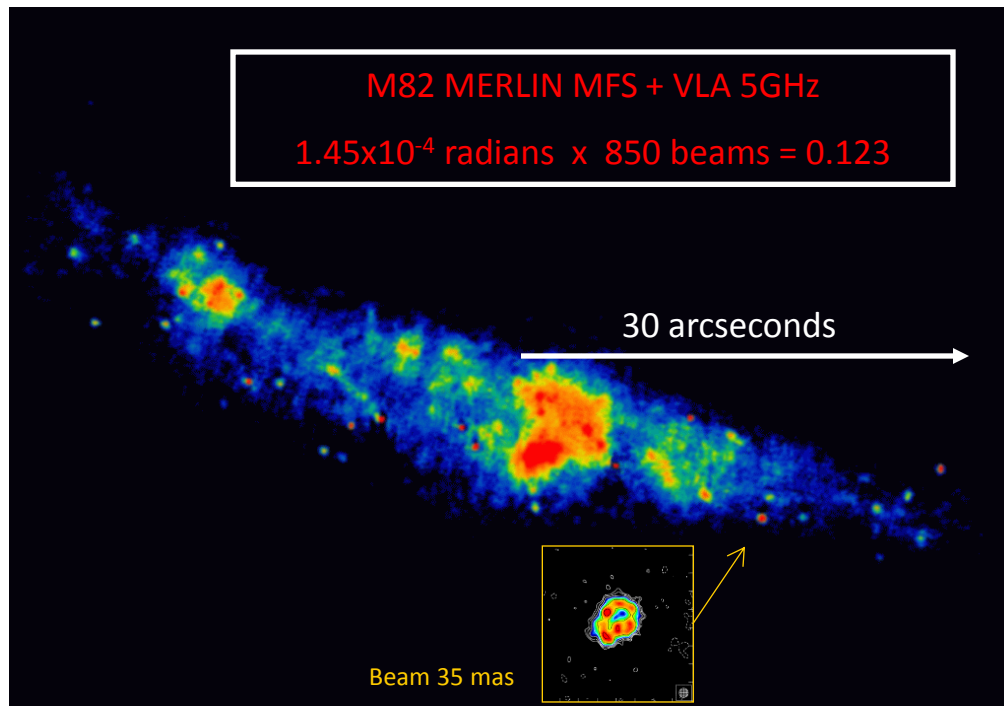
Bandwidth smearing (radial)

τ -averaging smearing (tangential)

Primary beam response

Wide-Field Imaging

Non-coplanar baselines



Standard Fourier synthesis assumes planar arrays – only true for E-W interferometers

Errors increase quadratically with offset from phase-centre

Serious errors result if

$$\theta_{\text{offset}}(\text{radians}) \times \theta_{\text{offset}}(\text{beams}) > 1$$

Need to account for a three-dimensional coherence function
 $V(u, v, w) \text{ FT} \rightarrow I(l, m, n) \text{ image vol.}$

– computationally expensive

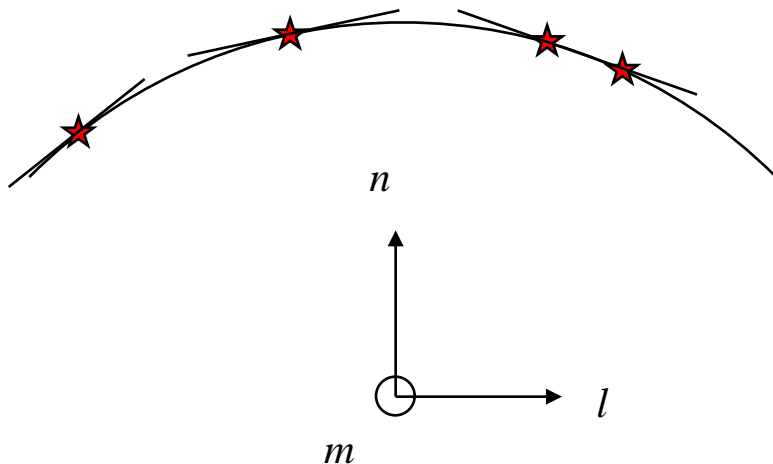
Wide-Field Imaging

Non-coplanar baselines

Computationally simple method of imaging \rightarrow a faceted or small field approximation in which the image sphere is approximated by pieces of many smaller tangent planes. The centre of each sub-field is correctly positioned in the three-dimensional image plane.

Within each sub-field fast two-dimensional FFTs may be used.

Errors increase quadratically away from the centre of each sub-field, but these are acceptable if enough small sub-fields are selected.



Facets can be selected so as to cover known sources.

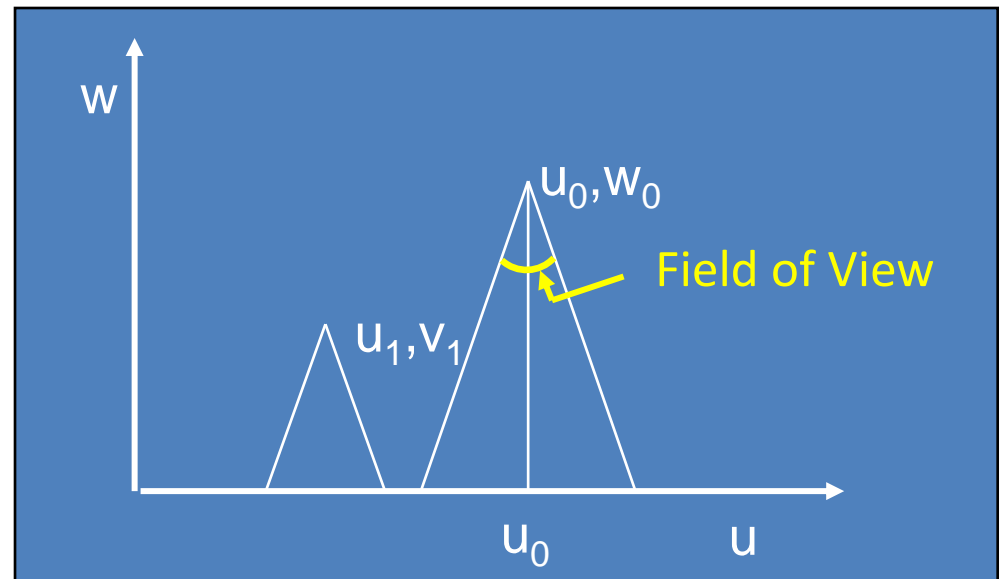
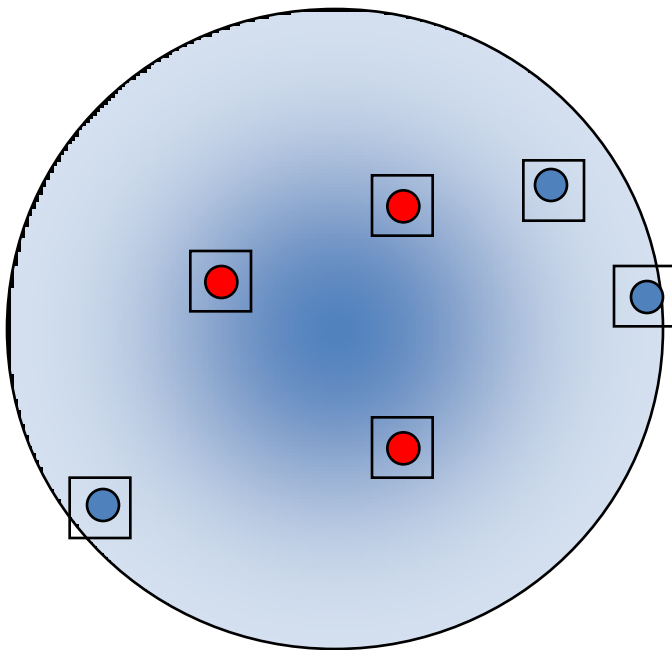
Facets may overlap allowing complete coverage of the primary beam.

Wide-Field Imaging W-Projection

An alternative to multiple facets has been developed: W-projection

W-projection allows the projection of each uvw visibility onto a single 2-D uv -plane ($w=0$) + phase shift proportional to the distance from the flat plane

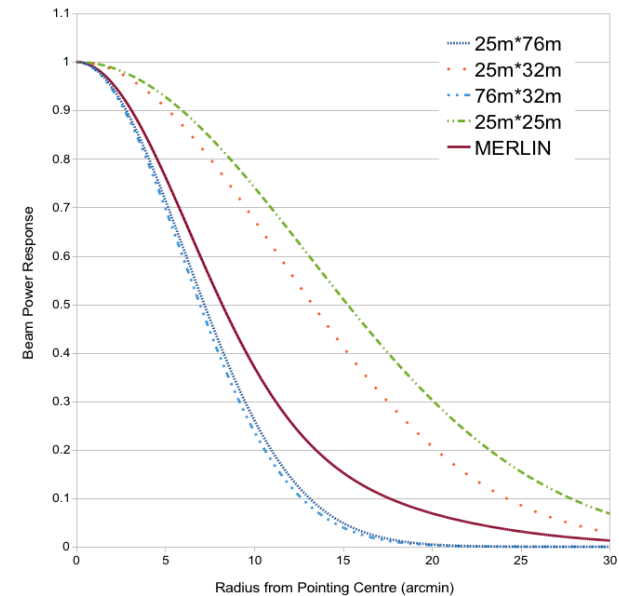
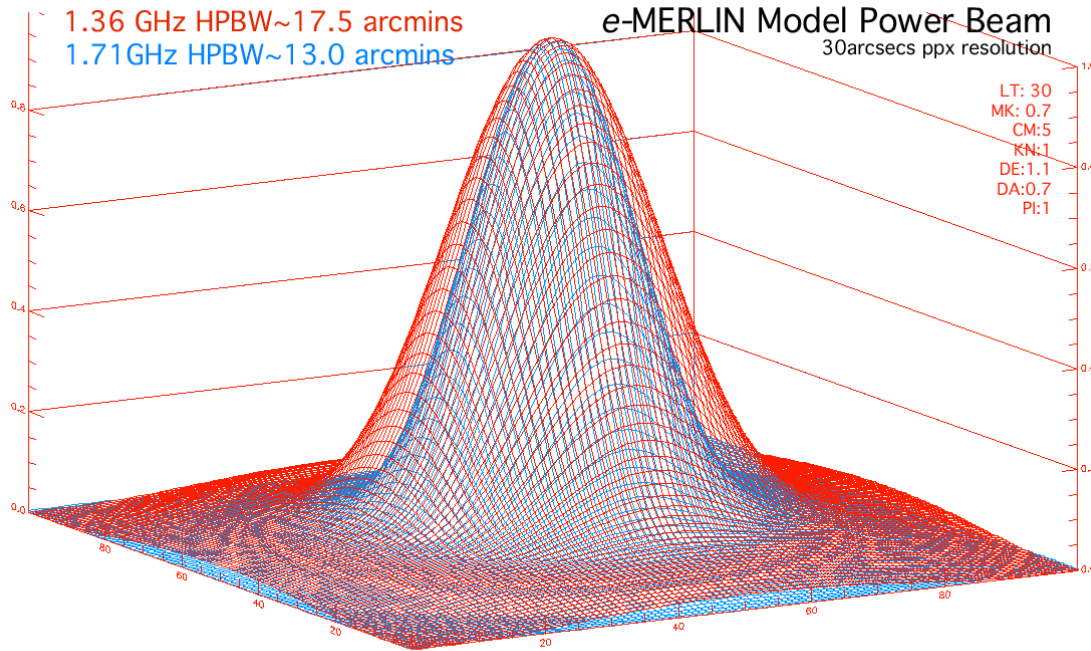
Each visibility mapped to all the uv points lying within a cone whose full angle is equal to the field of view of the required wide-field image



How big is the isoplanatic patch?
Direction-dependent corrections?

Wide-Field Imaging Primary beam response

The ultimate factor limiting the field of view is the diffraction limit of the individual antennas.



The overall correction will depend on the relative weighting and the data distribution between telescopes – & the types and sizes of the telescopes

Primary beam will be frequency dependent.

Radio Images

High resolution imaging of M87

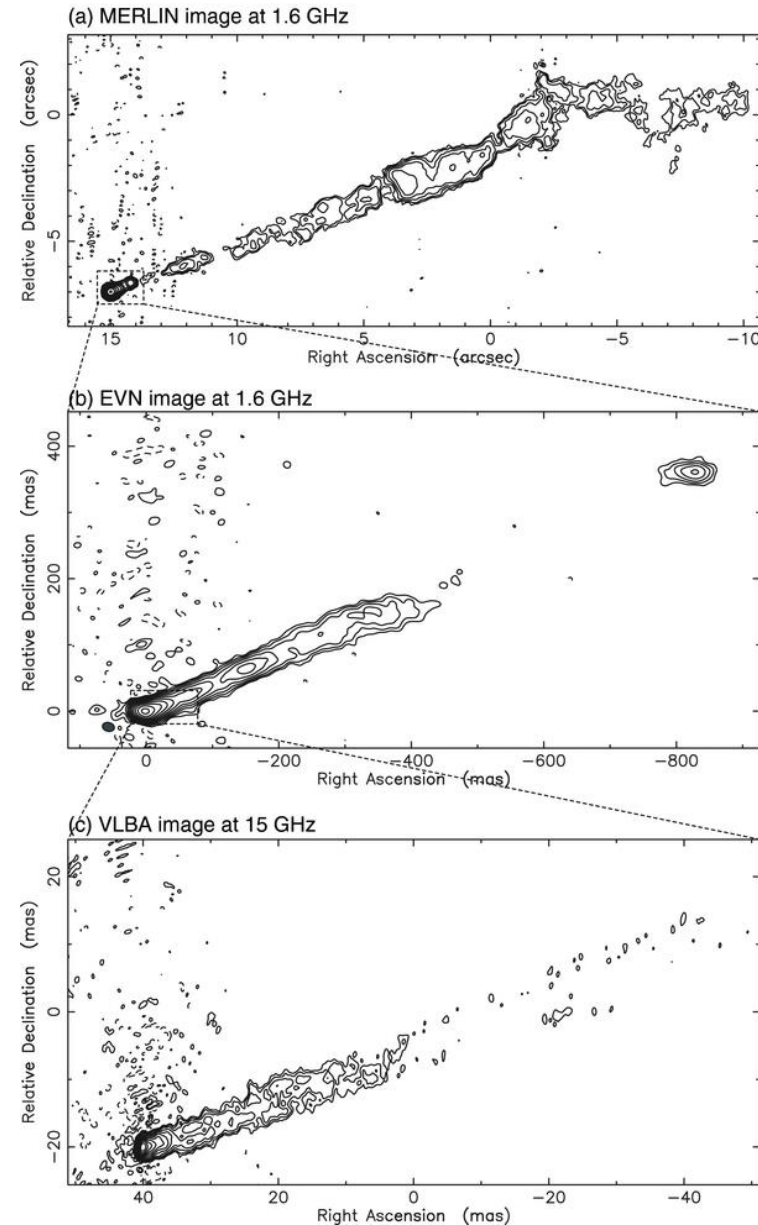
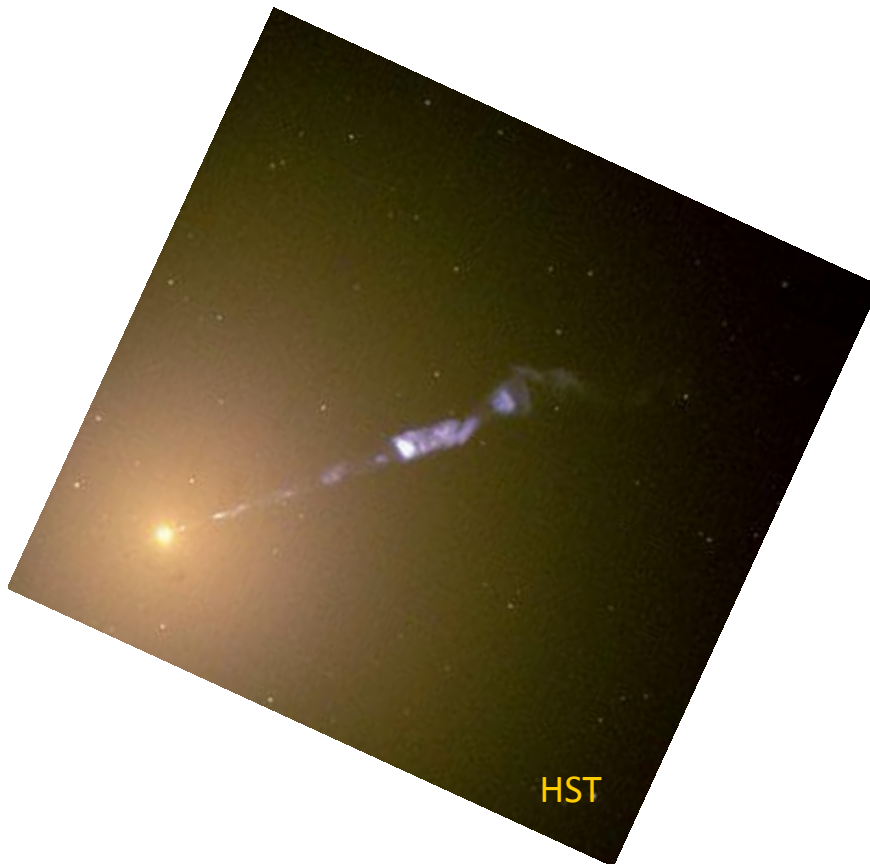
Merlin 1.6GHz data

EVN 1.6GHz data

VLBA 15GHz data

VLBA 43 GHz data

→ approaching the region of jet collimation?



Radio Images

High resolution imaging of M87

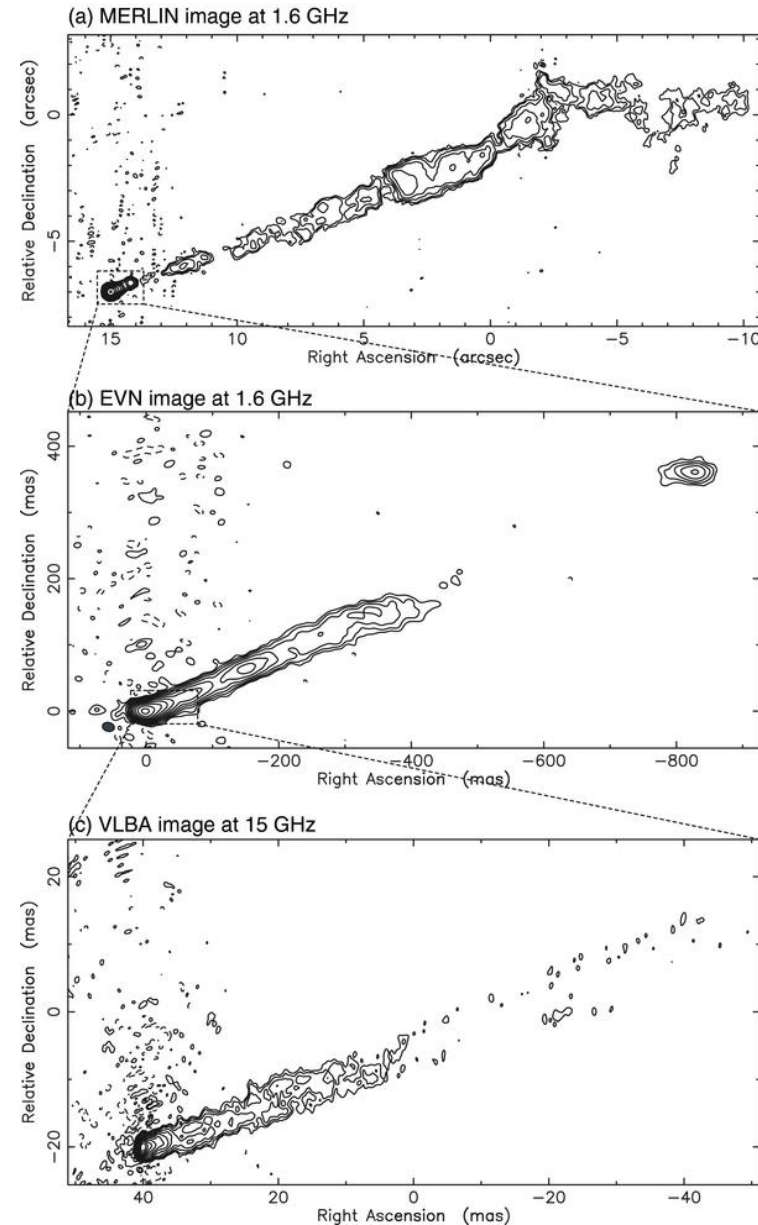
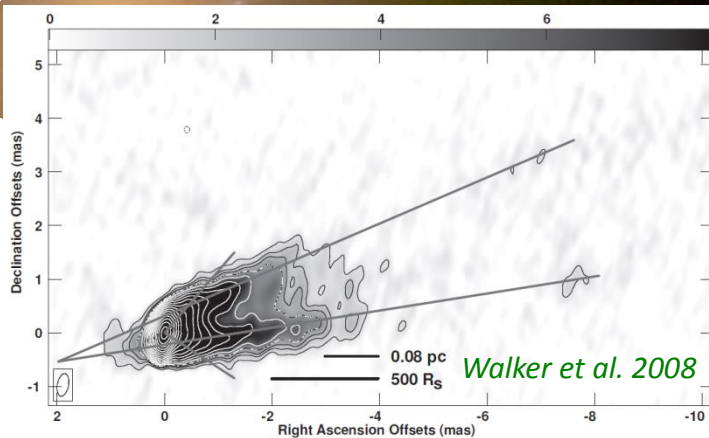
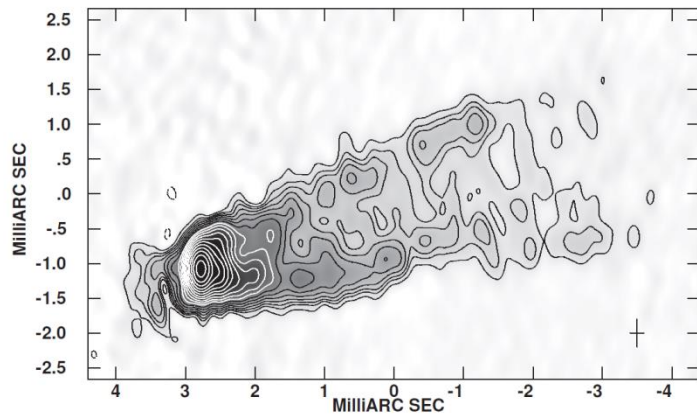
Merlin 1.6GHz data

EVN 1.6GHz data

VLBA 15GHz data

VLBA 43 GHz data

→ approaching the region of jet collimation?



Radio Images

High resolution imaging of M87

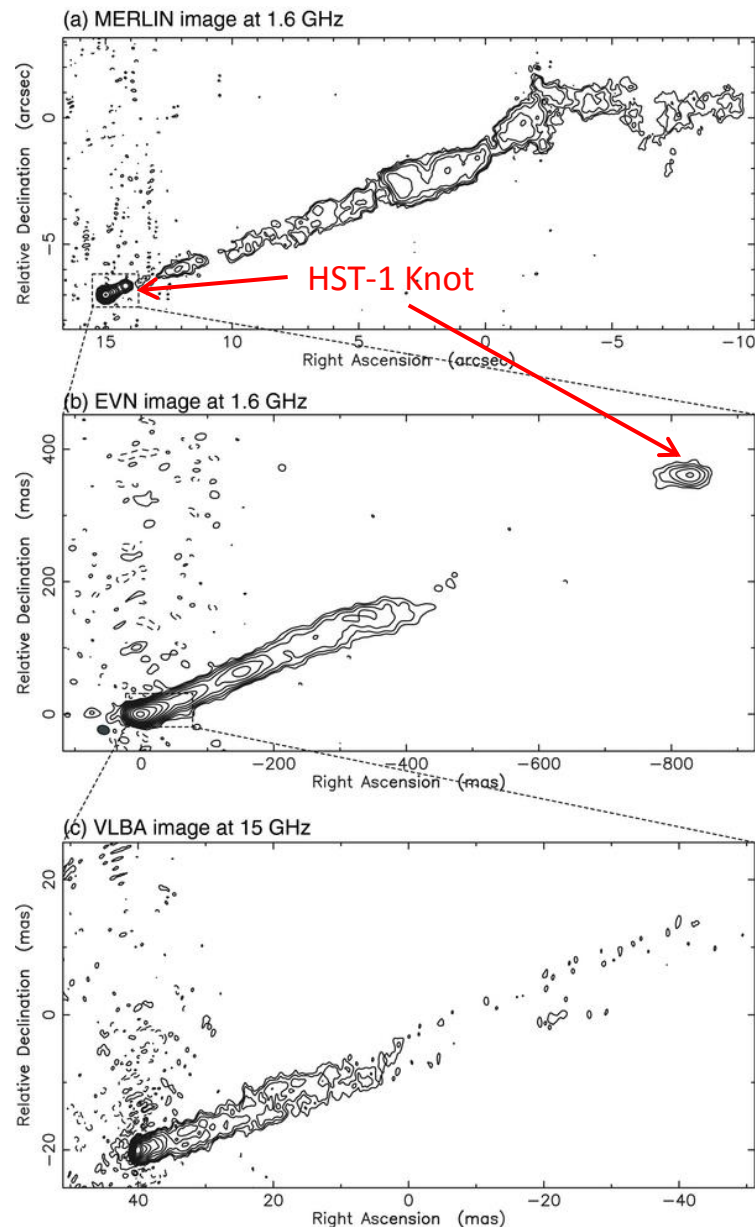
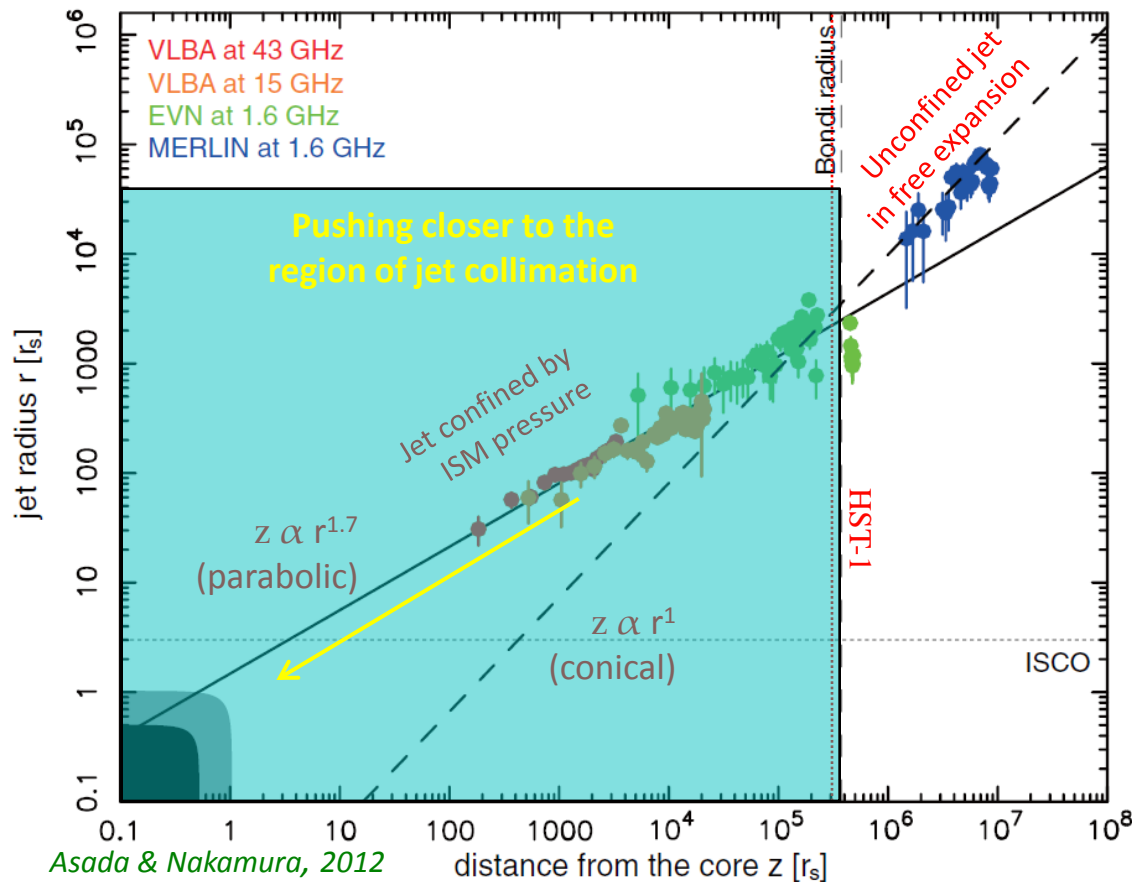
Gaussian fits to get jet widths

HST-1 lies near Bondi radius \rightarrow accreting gas goes supersonic

Upstream of HST-1 streamlines parabolic, downstream conical

Change in ISM pressure profile \rightarrow re-collimation shock

HST-1 knot is a stationary feature



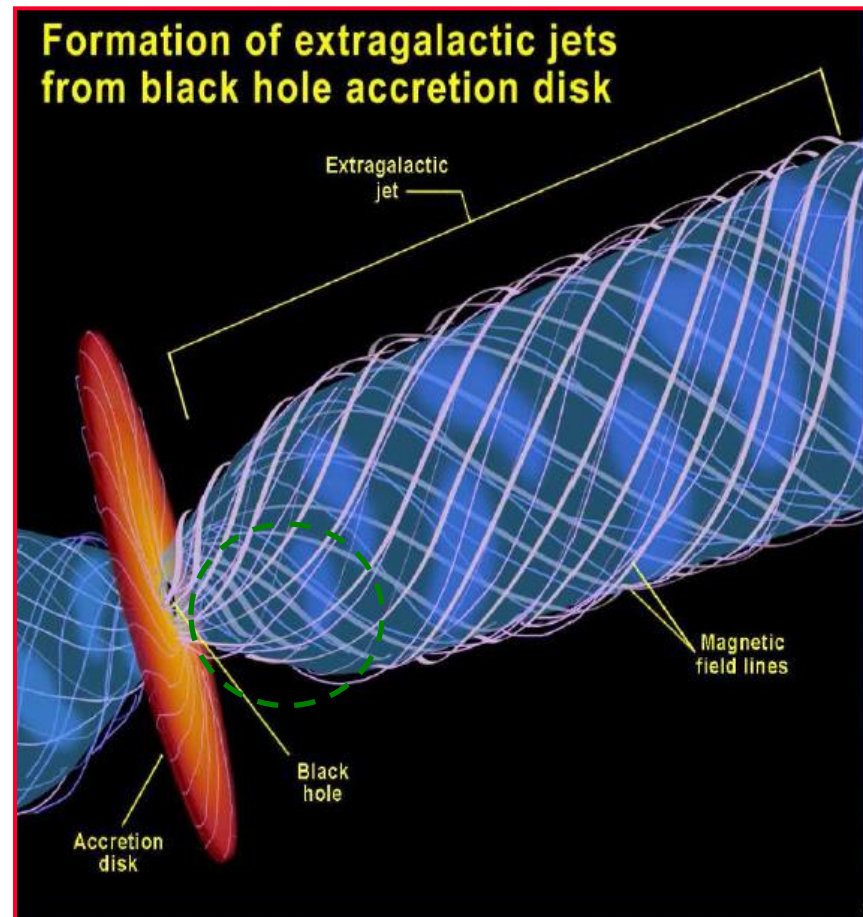
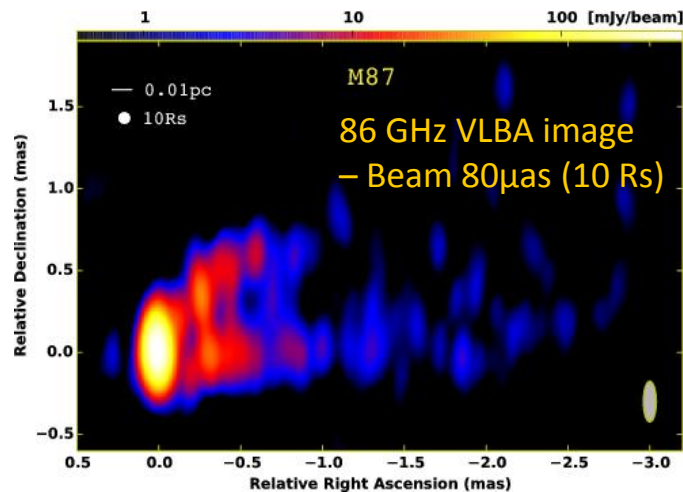
Radio Images

High resolution imaging of M87

Jet collimation region within $\sim 35 R_s$ de-projected distance along jet

Confirmed by 86 GHz VLBA

and 230 GHz mm VLBI imaging



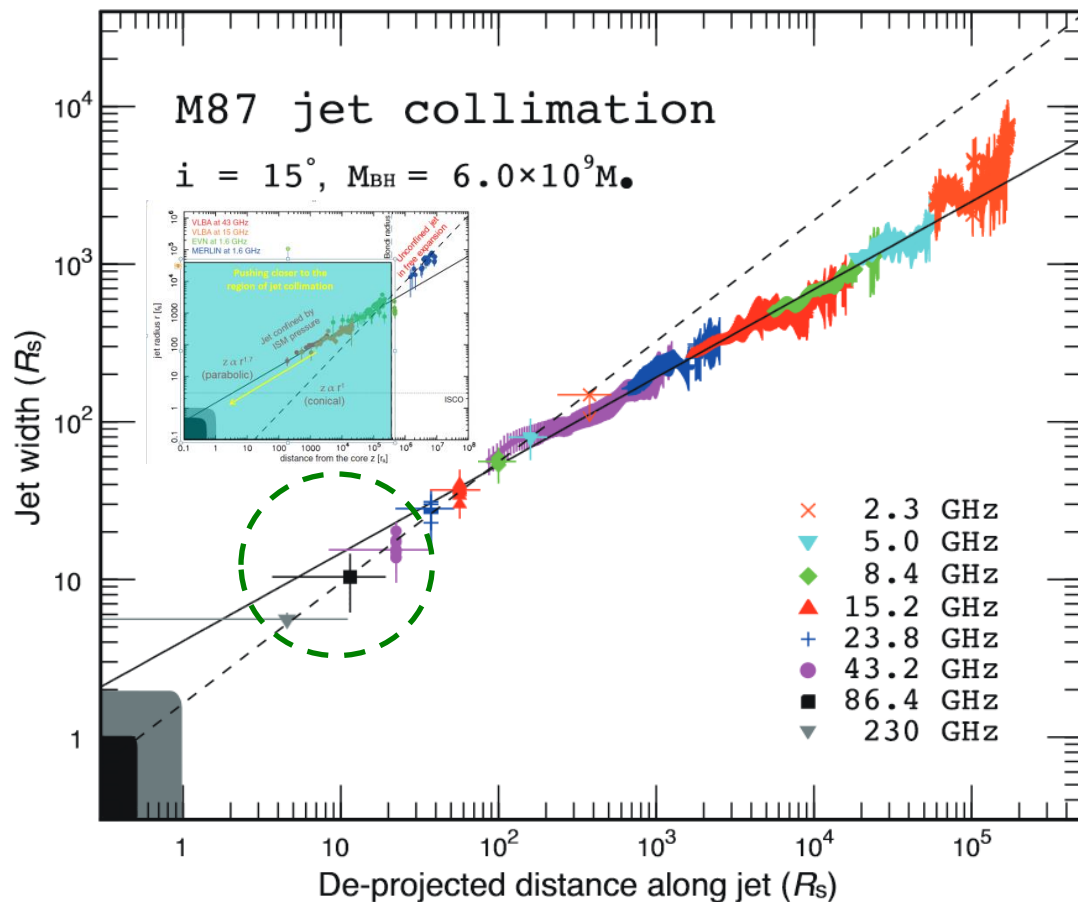
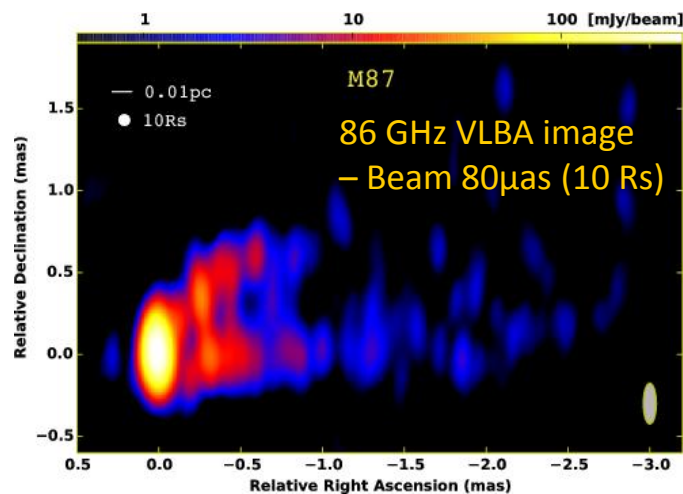
Radio Images

High resolution imaging of M87

Jet collimation region within $\sim 35 R_s$ de-projected distance along jet

Confirmed by 86 GHz VLBA

and 230 GHz mm VLBI imaging



Radio Images

High resolution imaging of M87

CARMA 10.4 m Cedar Flat, California
HHSMT 10m Mount Graham, Arizona
JCMT 15m Mauna Kea, Hawaii

CARMA-SMT

CARMA-JCMT

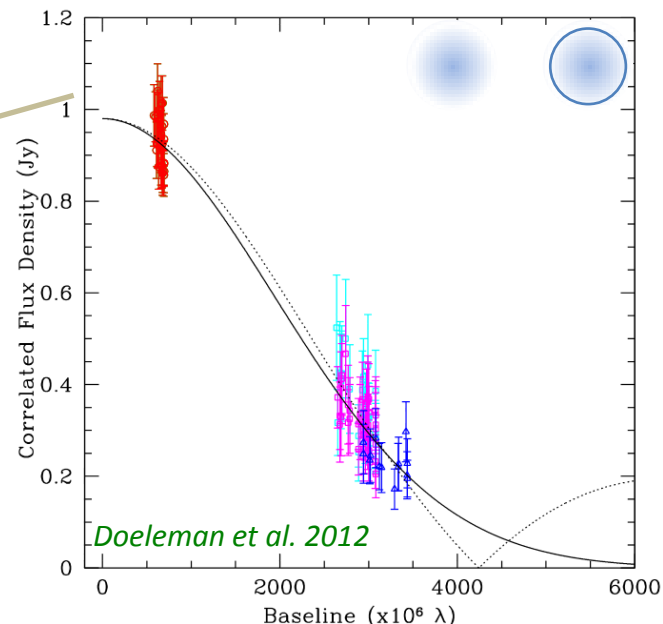
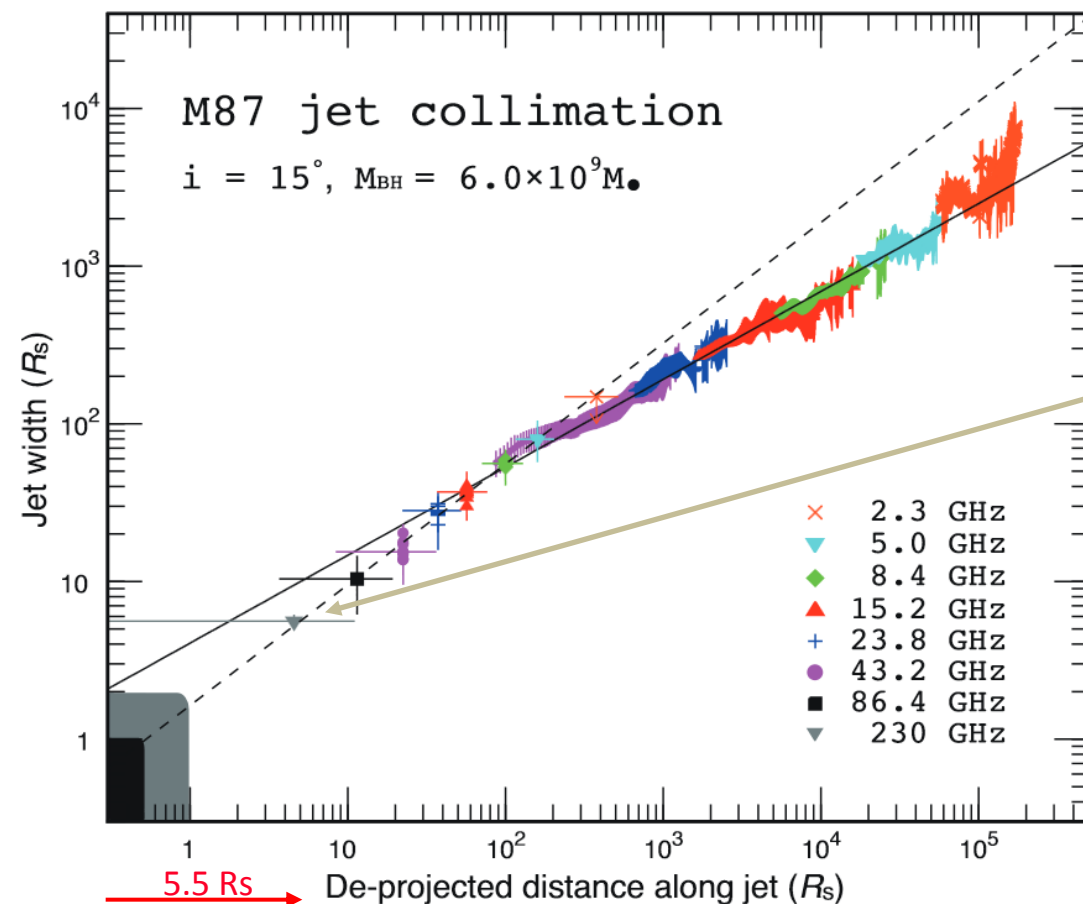
SMT-JCMT

Highest angular resolution study of M87
ever attempted ($3.5B\lambda$ at 1.3mm)

Fits to Amplitude

(No phase coherence)

- 40 μ s FWHM Gaussian (solid) &
- 40 μ s Gaussian + thin ring (dashed)



Radio Images

Event horizon telescope

Global sub-mm VLBI studies of nearby AGN systems (Sgr A* & M87)

Several mm-telescopes combined across the Earth

ALMA array to be phased-up for extreme imaging sensitivity

M87 $R_s = 7\mu\text{as}$ – with should be able to
image shadow of BH against background
counter-jet with $15\mu\text{as}$ resolution

Baseline	Resolution at 230 GHz	Resolution at 345 GHz
CARMA - SMT	300 μas	200 μas
Hawaii - SMT	58 μas	39 μas
Hawaii - ALMA	28 μas	19 μas
Plateau de Bure - South Pole	23 μas	15 μas



GR predicts that the shadow of a black hole should be circular (middle), but a black hole that violates the no-hair theorem could have a prolate (left) or oblate (right) shadow.

Future EHT images of nearby supermassive black holes will be able to test this prediction